"POLITEHNICA" UNIVERSITY from BUCHAREST
FACULTY OF MATERIALS SCIENCE AND ENGINEERING
Doctoral School of Materials Engineering

THESIS

Research on improving structural stability and oxidation resistance of INCONEL superalloys by rhenium addition

SUMMARY

Scientific leader:

Prof. Dr. Eng. Cristian PREDESCU

PhD student:

Eng. Andrei GRECU

Bucharest
2023

Content

INTRODUCTION

In the modern world, the development of technology has led to an exponential increase in requirements for advanced materials, capable of withstanding extreme conditions and intensive mechanical stress. Among these exceptional materials, Inconel superalloys are distinguished by their properties impressive, making them essential in the aerospace, energy, chemical and other industries technical. Inconel represents a family of nickel-based alloys, characterized by excellent resistance to high temperatures.

In the 1940s, research into the development of stronger and more durable materials led to the creation of the first nickel-based superalloys, known as "Inconel". Company American Special Metals Corporation (now part of the Special Metals Corporation group) was pioneer in the development of these high performance alloys. The term "Inconel" is, in fact, a registered trade name, but has become so widespread that it is generally used for a describes a wide range of nickel-chromium alloys, including those with various additions of molybdenum, cobalt, titanium and other elements. Currently, the industry uses several types of Inconel superalloys, the most used being Inconel 600, Inconel 625 and Inconel 718.

Inconel superalloys are distinguished by a unique combination of properties that make them suitable for critical applications in extreme environments. One of their defining traits is endurance at high temperatures. These alloys retain their structural strength even at temperatures that exceed 1000°C, making them ideal for components that operate under temperature conditions such as aircraft turbines or thermal and nuclear plant equipment. Of also, the presence of nickel in high proportions gives these alloys excellent resistance to corrosion, which makes them suitable for applications in acidic, alkaline and salty environments.

In addition, Inconel superalloys are characterized by outstanding mechanical strength and o good ductility, which allows the manufacture of complex parts and structures with rigorous requirements strength and reliability. They also have good machinability and can be easily welded, facilitating the production of customized components for various industrial applications. In the overall, the combination of these properties makes Inconel superalloys essential for aerospace industry, energy industry, chemical and petrochemical industry, medicine and dentistry, the defense industry and many other areas where reliability and durability are crucial.

The doctoral thesis proposes the design, elaboration, thermal treatment and physical characterization structural of a number of five Inconel superalloys, of which 4 with variable rhenium content.

Head. 1. GENERAL ASPECTS REGARDING THE NOTION OF SUPERALLOY

1.1. Overview

Superalloys are special materials rich in at least one of the elements nickel, cobalt or iron, which maintain the structural stability of the surface and the physical-mechanical properties at high temperatures, under high stress and in severe environment.

Due to these qualities, superalloys are widely used in industrial fields of top, such as aeronautical industry, nuclear industry, space industry, energy industry, etc.

Superalloys are alloys resistant to high temperatures, featuring a combination of mechanical strength and resistance to surface degradation [1]. In fact, they are mainly used at engines in the aerospace industry, in gas turbines, combustion plants and in the chemical industry and energy, for other special applications, which require resistance to high temperatures and/or to corrosion, i.e. primarily possessing refractoriness properties. A remarkable feature of of nickel-based alloys is their use in load-bearing applications at temperatures exceeding 80% of their starting melting temperature, a fraction that is higher than for any other class of alloys.

1.2   Classification   of   superalloys

Superalloys are classified into several categories depending on the predominant metal present in alloy. Thus there are:

- Nickel-based superalloys

- Titanium-based superalloys

- Cobalt-based superalloys

- Iron-based superalloys

1.2.2   Nickel-based   superalloys
Nickel-based superalloys are the most complex, the most widely used for fields where the working conditions are very complex: high temperatures associated with important mechanical demands. Some authors consider them the most interesting of all superalloys [3], but obviously, their point of view can be considered subjective by other specialists. They currently make up over 50% of the weight of advanced aircraft engines. The main characteristics of nickel as a base in these alloys are the advanced mechanical properties (association favorable balance between mechanical resistance and plasticity), a remarkable creep behavior and o advanced resistance to both electrochemical corrosion and oxidation, i.e. dry corrosion, marked by high temperatures. A favorable characteristic of nickel is its data crystallographic, its crystallization system being face-centered cube (CFC) the most favorable cell BRAVAIS, which ensures even from the crystalline level the most advantageous properties. By alloying

nickel forms a series of solid substitution solutions with important mechanical properties, achieved through the dissolution hardening mechanism.

The most important use of Ni-based superalloys is in the manufacture of gas turbines, encountered in the construction of turbojets from commercial and military aircraft, in subassemblies energy generators in the energy industry or in the propulsion subassemblies of ships marine.
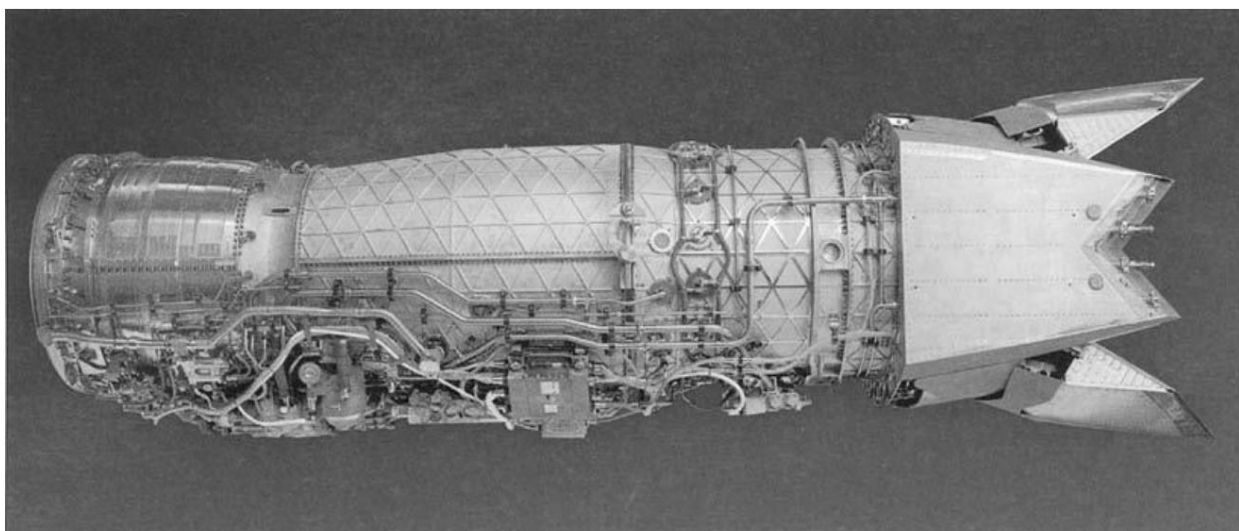
Figure 1.2. F119 gas turbine engine; a major user of superalloys [7]

1.4.2.2 Melting processes

The traditional processes used to produce superalloys are shown in Figure 1.6.
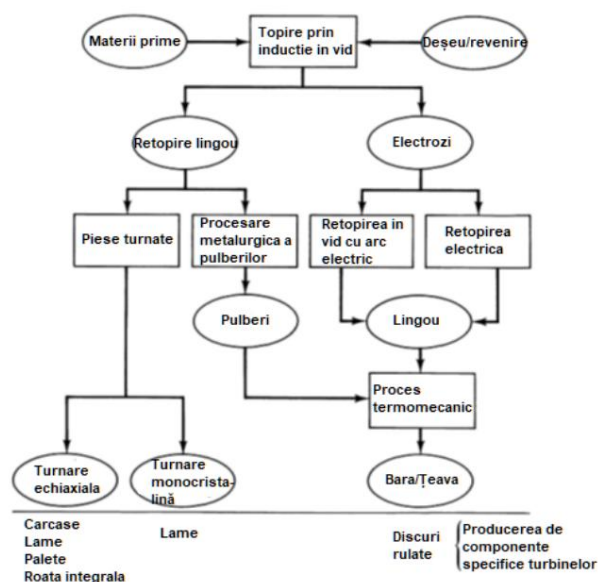
Figure 1.6. Widely used technologies for the production of superalloys [7]

1.4.3 Superalloys obtained by powder metallurgy

To increase the strength of polycrystalline Ni-based superalloys, the addition levels refractory alloys and the forming elements of the ÿ' phase gradually increased to levels that make ca

7

conventional processing routes to be deficient [18]. Elements such as W, Mo, Ti, Ta and Nb effectively harden the alloy, but also lead to severe ÿ solid solution segregation. In addition, the limited ductility of high-strength alloys makes the ingot susceptible to cracking as thermally induced stresses evolve during cooling. Powder processing routes have been developed to overcome the difficulties associated with melt defects and are viable for the production of advanced high-strength polycrystalline superalloy components. They are listed in Table 1.1 the compositions of Ni-based superalloys processed with commercially available powder [19].

Powder processing begins with gas or vacuum atomization of a highly alloyed VIM ingot. The rapid solidification of fine powders effectively suppresses macrosegregation in the alloy.

Head. 2. THE CURRENT STATE OF KNOWLEDGE IN THE FIELD OF STRUCTURE AND MECHANICAL PROPERTIES AT HIGH TEMPERATURES OF ALLOYS

INCONEL alloy

2.1. The structure of Inconel type alloys

The first analysis of INCONEL alloys, in which the basic element is nickel, and the main chromium alloying element is made by studying the Ni-Cr equilibrium diagram fig. 2.1). It remains of interest the domain on the nickel side, where the alloys in this category are found.
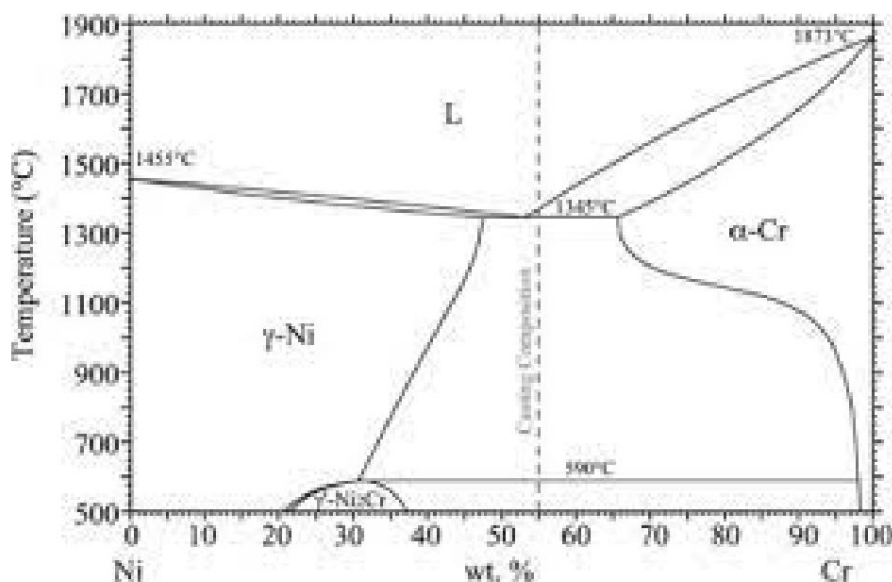
Fig. 2.1. Ni-Cr phase equilibrium diagram [128]

In general terms, the equilibrium diagram falls into the category of those with total solubility in liquid state, partial solid state and eutectic transformation. The wide variations of the solvus lines, which indicate the possibility of applying heat treatments of hardening for laying in solution and artificial aging for alloys whose vertical composition lies below these. The effect will primarily be that of increasing mechanical performances through the mechanism of hardening by precipitation.

8

2.2. Comparative study on the influence of the manufacturing process of superalloys Inconel on structure and mechanical properties

One of the most commonly used alloys with applications in aeronautics, gas turbines, turbocharger rotors and a variety of other corrosive and structural applications involving temperatures up to ~700° C, it is Inconel 718.

Table 2.1. Chemical composition of Inconel 718 alloy

Element	Ni(%)	Cr (%)	Nb (%)	Mo(%)	TI(%)	Co(%)	Al(%)	Fe(%)
(%)	50-55	17-21	4.8-5.5	2.8-3	0.6-1.1	1	0.2-0.8	dif

The alloy is designed for tensile strength, creep resistance and good durability at fatigue at high temperatures up to 700°C and is known to have a weldability good due to its relatively slow precipitation kinetics [25], [26].

The microstructure of Inconel 718 contains a solid solution matrix ÿ (A1) with a fair amount of primary carbides and intermetallic phases of the Ni3Me type, namely ÿÿ Ni3(Al,Ti,Nb) (L12), ordered tetragonally ÿÿ Ni3Nb, and CFC MX (Nb,Ti)(C,N). The microstructure could include, de also compact unwanted phases such as hexagonal Laves (Ni, Fe, Cr)2(Nb, Mo, Ti), orthorhombic ÿ Ni3(Nb, Ti) and tetragonal ÿ CrFe phases [27] (Fig. 2.2).
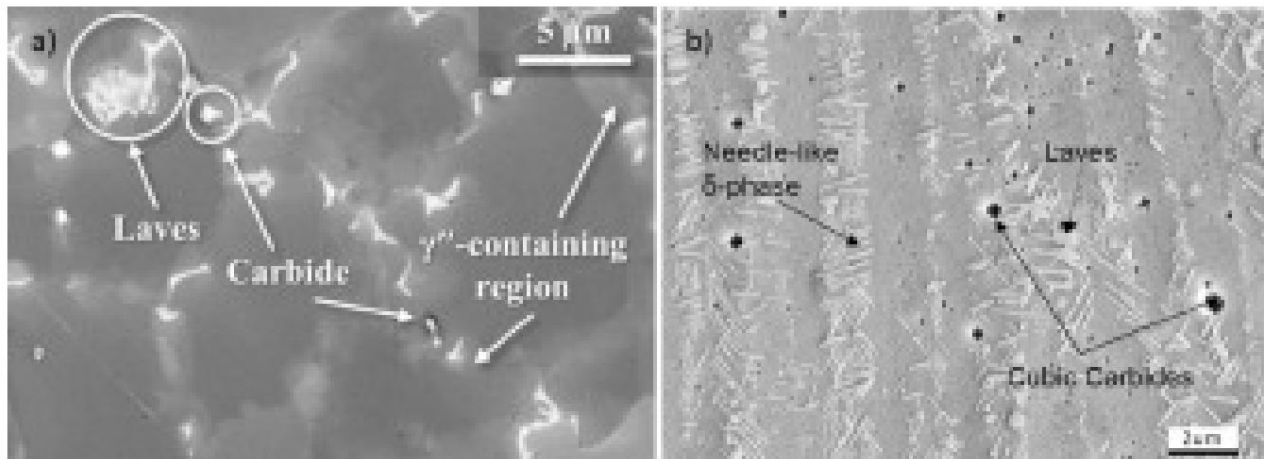
Fig. 2.2. Main precipitates in Inconel 718: a) interdendritic Laves phase, NbC carbides and bright regions containing ÿÿ in direct laser deposited (DLD) Inconel 718 [28]; b) Laves, cubic carbides and needle-like ÿ-phase in thermally treated selective laser melted (SLM) Inconel 718 [29]

The main toughening phases for Inconel 718 are bond metastable ÿÿ and ÿÿ coherent and semi-coherent with the ÿ CFC matrix.Alloy Additive Manufacturing (MAM) is an advanced manufacturing method that allows building three-dimensional (3D) parts, layer by layer, either from powder or from feed material from wire, with good accuracy and directly from a CAD model, without special tools or knowledge of the piece [30], [35].

Fig.2.3 shows schematic views of different MAM techniques.
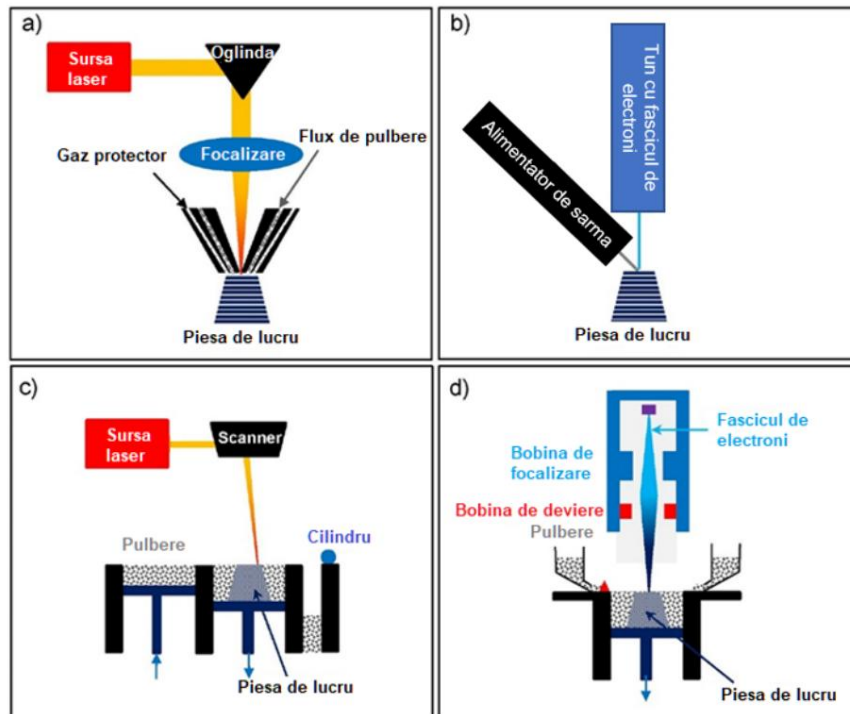
Fig. 2.3. *Schematic of different MAM processes, (a) direct laser deposition (DLD); (b) direct electron beam (wire) deposition (DEBM); (c) selective laser melting (SLM) and (d) electron beam melting (EBM) [39].*

The sensitivity of the microstructure (and consequently the mechanical properties) of AM is based on the AM scanning strategy and beam parameters that promote the ability to achieve control site-specific microstructure within a manufactured component [61], [62], [63]. An Inconel AM Functional 718 was produced with different fine- and coarse-grained microstructure regions (Fig. 2.7) [62]. Variation of the microstructure has been shown to have a direct influence on the properties local mechanics and a steep hardness gradient between zones was observed
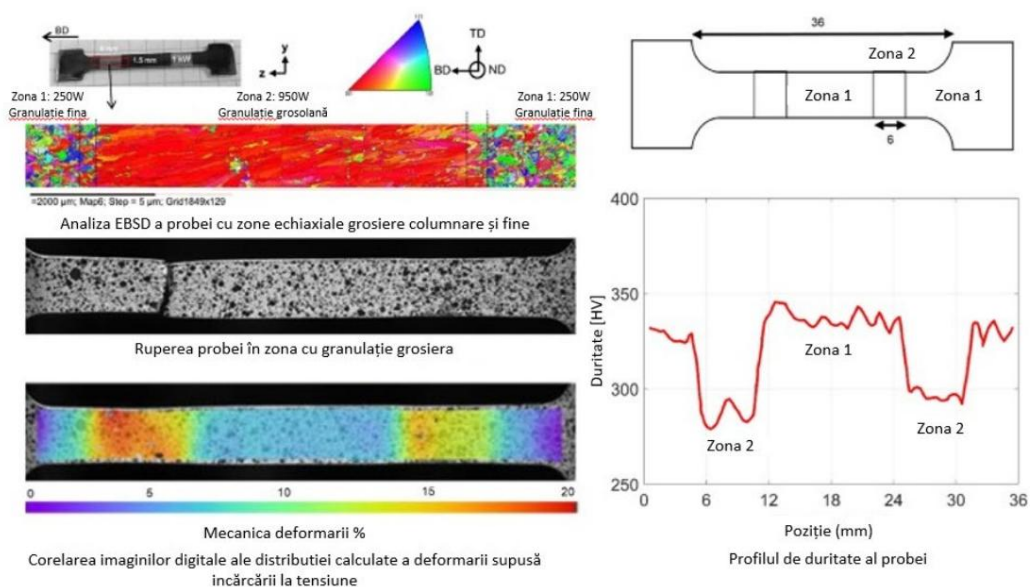
Fig. 2.7. *Microstructure, hardness profile and strain distribution under tensile load for a functional AM Inconel 718 [62].*

2.4. The effect of heat treatment on the microstructure of Inconel 718

For AM Inconel 718, the as-built microstructure contains the brittle Laves phase and the ÿ phase which forms mainly due to the micro-segregation of Nb and Ti [64], [73], [74]. The goal of the solution quenching heat treatment for AM Inconel 718 is phase dissolution Laves and ÿ and homogenization of Ti, Al and Nb distribution in the matrix. This helps with precipitation effective of fine ÿÿ and ÿÿ and reaching the maximum strength in the subsequent aging treatment [61], [64], [75].

After the homogenization/solution treatment, the main hardening phases of ÿÿ and ÿÿ se form during subsequent aging treatments [73], [74], [79], [80]. Double treatment of aging after solution treatment/homogenization at 1080°C resulted in strength and ductility of 1529±19MPa and 18.6±0.9% for AM Inconel 718, which are superior to those for Inconel 718 forged [81]. Fig. 2.8 shows the microstructure of SLM Inconel 718 under different treatment conditions thermal. Due to the rapid solidification and high cooling rate during SLM processes, the precipitation phases with hardening effect is largely inhibited. Therefore, the extent of precipitation such as ÿÿ and ÿÿ is significantly decreased under construction conditions, leading to a decrease in a mechanical strengths of the alloy [27], [82], [49], [83].
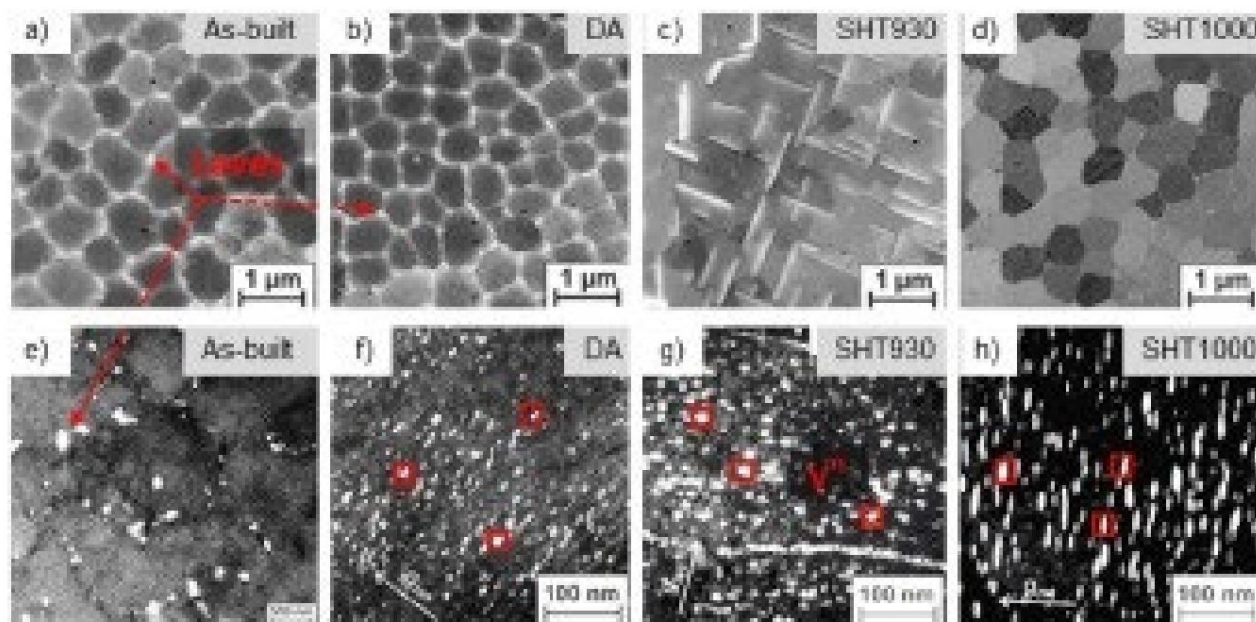
Fig. 2.8. (a–d) *scanning electron microscopy (SEM) images and (e–h) dark-field transmission electron microscopy (TEM) images characterizing the microstructure of SLM Inconel 718 after different heat treatment processes [49].*

2.8. ConCluSIonS

- Inconel 718 is one of the most frequently used alloys for additive manufacturing metallic (AM) and has a wide range of applications in aircraft, gas turbines, rotors of turbochargers and a variety of other corrosive and structural applications up to ~700°C.

- Due to rapid solidification and high cooling rates during AM processes, the as-built AM Inconel microstructure consists of a supersaturated ÿ matrix, phase Laves and a limited amount of hardening particles ÿÿ and ÿÿ.

Head. 3. METHODS AND METHODOLOGY, ANALYSIS TECHNIQUES FOR ACHIEVEMENT OF OBJECTIVES

3.1. The purpose and objectives of the research

The main aim and objective of the research is the design and realization of nickel-based superalloys, of which 4 (P2-P5) with variable rhenium content, with superior physical and mechanical properties, with uses in the aerospace, energy, chemical and defense industries. In this sense, the research direction will go through the following steps:

- analysis of data from the specialized literature regarding nickel-based superalloys;

- the development of five types of superalloys, of which two exist in current technologies and three containing rhenium;

- the comparative analysis of the structure of the five superalloys after elaboration in vacuum and atmosphere of argon;

- performing heat treatments on the developed superalloys and investigating the structures obtained;

- comparative analysis of the structure of the five thermally treated superalloys;

- the physico-mechanical characterization of superalloys with rhenium content compared to the two existing superalloys, in all phases: elaboration, heat treatment;

3.2. Research methodology

To establish the research methodology, the current state of the of research in the field of nickel-based superalloys, found after studying the literature of specialty. Alloying elements such as Co, Cr, Mo, Re, Ta, Ti, W are added to enhance

the properties of increasing corrosion resistance at high temperature. Among these elements of alloys, Re mainly improves corrosion resistance and creep resistance remarkably [3,4].

Based on what was presented, the research plan was drawn up considering the following aspects:

1) Justification of the need to approach the research theme, as an important subject of science materials, with emphasis on behavior at high temperatures and heavy tribological conditions;

2) Contributions to the development and improvement of some processing technologies and thermal treatments of superalloys with nickel base and rhenium content;

3) Contributions to obtaining homogeneous structures with physical-mechanical properties superior.

Through this objective, the possibilities of elaboration and heat treatment are scientifically substantiated of nickel-based superalloys used in the aerospace, energy and defense industries.
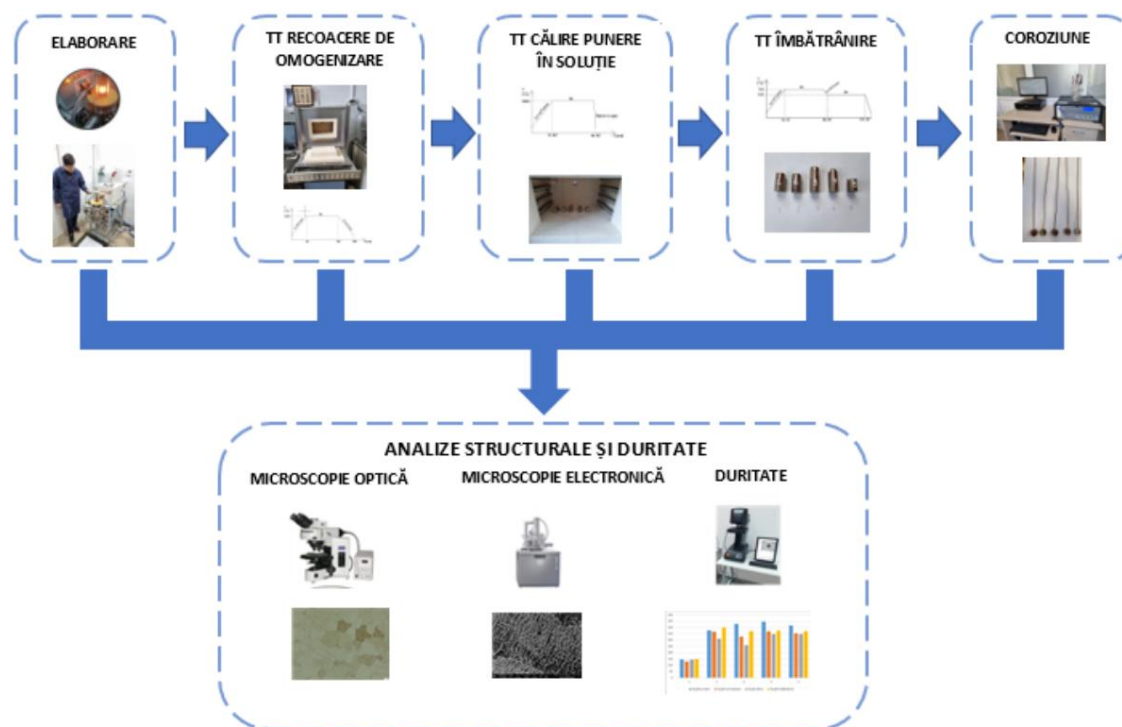
Fig. 3.1. *The structure of the doctoral thesis research plan*

3.3. Experimental research

Experimental research consisted of fundamental and applied research activities.

Methodologically, the realization of the research was taken into account, depending on **the content and the destination superalloys made,** as follows:

3.4. Materials used in research

During the research, 5 types of nickel-based superalloys were developed, of which 4 new, of own design, with variable rhenium content.

Materials with the composition shown in table 3.1 were used for their development.

Table 3.1 *Chemical composition of materials used in the development of superalloys[128]*

Material	c (%)	Nb (%)	Mo (%)	IT (%)	the (%)	Fe (%)	w (%)	-R (%)	us (%)	Re (%)	Co. (%)	Your (%)
us	-	-	-		-	-	-	-	99.99 -		-	-
IT	-	-	-	99.99	-	-	-	-	-	-	-	-
-R								99.9				
the	-	-	-	-	99.9 -		-	-	-	-	-	-
CMSX4 -		-	0.60	1.0	5.6 -		6.0	6.50 diff		3.0	9.0	6.5
AMCO 0.005 -			0.043		0.00 diff	-		0.00 0.01		-	-	-
INCONEL alloy 625	-	3.85	8.5	0.2	0.35 4.63 -			22.5 diff		-	0.24	-

3.5. Development of nickel-based superalloys for experimental research

The five categories of INCONEL superalloys used for experimental research were developed in a cold crucible levitation furnace, in vacuum and controlled atmosphere (argon), of the Fives type Celes ALU 600, in the equipment of the ECOMET center.

3.6. Thermal treatment of developed superalloys

The heat treatments of the elaborated superalloys were done in the heating furnace NABERTHERM, provided by the ECOMET Center.

3.7. Analysis techniques used to carry out research

3.7.1. Chemical composition analysis

Determination of the chemical composition of the developed superalloys for experimentation and verification fitting into the previously established chemical composition, was done with the Leco optical emission spectrometer GDS 500 A.

3.7.2. Metallographic analysis by optical microscopy

Microscopic analysis to identify constituents and possible defects and imperfections resulting from the process of elaboration and casting was achieved by using a microscope Olympus BX 51M. The microscope was part of the ECOMET Center in UPB.

To highlight the microstructure of the superalloys, the samples were subjected to attack metallographic with Marble reagent.

3.7.3. Microstructural and microcompositional analysis -

by electron microscopy of scanning electron microscope (SEM) and energy dispersive X-ray microanalysis (EDAX). with sweeping Model QUANTA 450 FEG, with the following characteristics:

3.7.4. Determination of hardness

The determination of the hardness was done with the Innovatest Falcon 500 automatic hardness tester, for microhardness measurement;

3.7.5. Determination of corrosion resistance

To study the corrosion behavior of the five elaborated superalloys, a potentiometer/galvanostat brand Gamry Reference 600 having a specialized data analysis software purchased Echem Analisys, located in the endowment of the corrosion laboratory at the Faculty of Industrial Engineering and Robotics from UPB. A classical electrochemical cell with three was used electrodes, the working-sample electrode, the platinum counter electrode and the reference electrode - the electrode saturated with calomel.

Head. 4. DEVELOPMENT OF INCONEL SUPERALLOYS IN VACUUM INDUCTION FURNACE AND ARGON ATMOSPHERE AND THEIR CHARACTERIZATION; HOMOGENIZATION BY ANEANING

In order to carry out the experimental research, 5 types of INCONEL superalloys were developed, which

they were subsequently subjected to the processes of heat treatments, determination of hardness and characterization

physical-structural.

4.1. Chemical composition selection for Inconel superalloys

In order to carry out the experimental research, 5 types of INCONEL superalloys were developed. The alloying elements present in their chemical composition - Al, Nb, Mo, Ti, Co, Ta, W, Re, were chosen so as to ensure the classic technological characteristics for which they were developed and on on the other hand, to improve the operating characteristics at temperatures in a modern way raised.

4.2. The choice of alloy compositions and raw materials used in the elaboration
Inconel superalloys

To obtain the superalloys analyzed in this paper for the calculation of the load have

used raw materials with known and verified chemical compositions, presented in table 3.1, chapter 3.

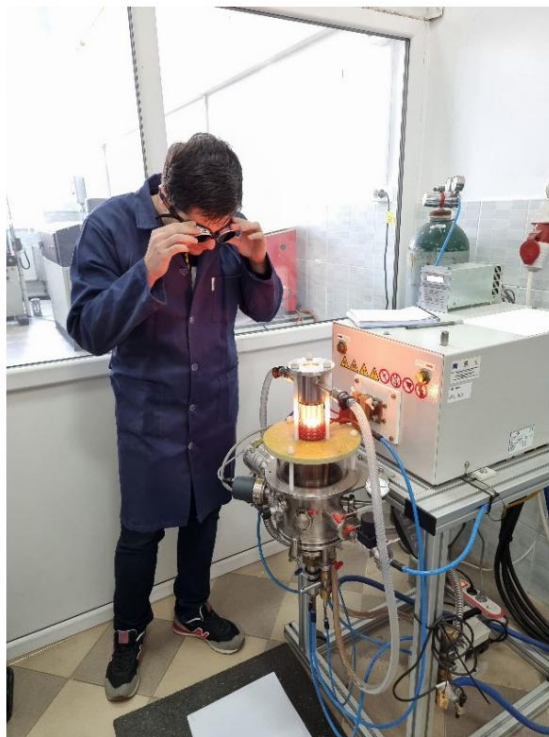***Fig.4.1*** *Vacuum induction cooking furnace with cold crucible and argon atmosphere*

The compositions of these superalloys are presented in table 4.1.

It should be noted that the compositional proportion of the Inconel superalloys was chosen taking into account

of the influence of each alloying element, on the physical-mechanical properties, but especially of

corrosion resistance at high temperatures.

Table 4.1. *Composition of developed Inconel superalloys, in mass*

Material	Al(%)	Mo(%)	Cr (%)	Ni (%)	Ti(%)	Si(%)	Fe(%)	Nb(%)	Ta(%)	W(%)	Re(%)	C(%)	Co(%)
Proba 1	1,75	-	22,2	73,26	-	1,26	1,51	-	-	-	-	0,02	-
Proba 2	3,85		12,67	66,43	1,16	0,08	0,83	-	4,60	2,84	1,6	0,03	5,91
Proba 3	5,20	0,58	6,92	63,04	1,49	-	-	-	6,58	4,34	1,96	0,02	9,87
Proba 4	8,27	0,56	6,47	60,06	1,45	-	-	-	6,27	4,31	2,98	0,02	9,61
Proba 5	5,43	2,71	12,62	64,28	0,79	-	1,76	0,76	3,38	1,28	1,02	0,03	5,89

The alloys were developed in a vacuum, and the melt was protected during ingot casting by using a controlled argon atmosphere. The materials used for the elaboration were preheated to 250°C to remove moisture, in an ordinary heating oven, existing in the center's research laboratories.

The developed samples are presented macroscopically in figure 4.2.
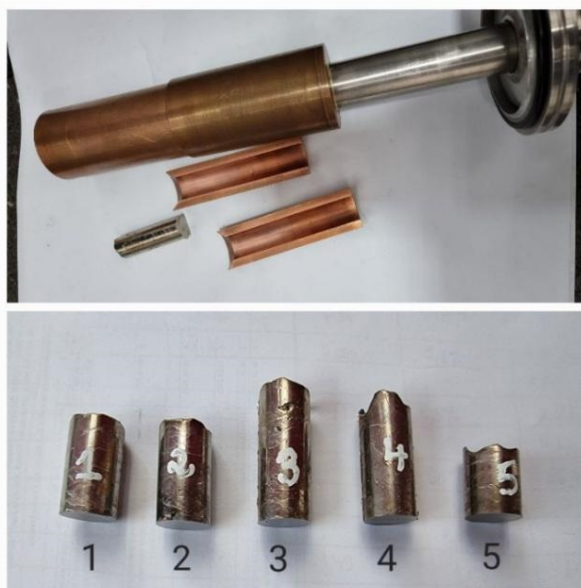
Fig. 4.2. *The ingots of superalloys obtained during processing in the induction furnace*

4.3. Determining the hardness of alloys after working-casting

Following the centralization of the results of the hardness test after the development of the superalloys, it is found that sample 1 has the lowest hardness, 146 HV2, with values between 143 and 148 HV2, followed by sample 2, with a mean value of 378 HV2 and values ranging from 362 to 386 HV2. For the test 3 hardness figures range between 328 and 451 HV2 and mean value 428 HV2, sample 4 records values between 433 and 454 HV2, with an average value of 445 HV2 and finally, sample 5 brings hardnesses between 405 and 417 HV2, the average value being 416 HV2.

4.4.1 Structural analysis by optical microscopy

Following the development of the Inconel superalloys, the 5 experimental samples were prepared for metallographic examination by optical microscopy.

In fig. 4.4, fig. 4.5, fig. 4.6, fig. 4.7 and fig. 4.8 optical microscopy images are inserted analyzed.

The purpose of these investigations was to observe the structure obtained directly after casting.
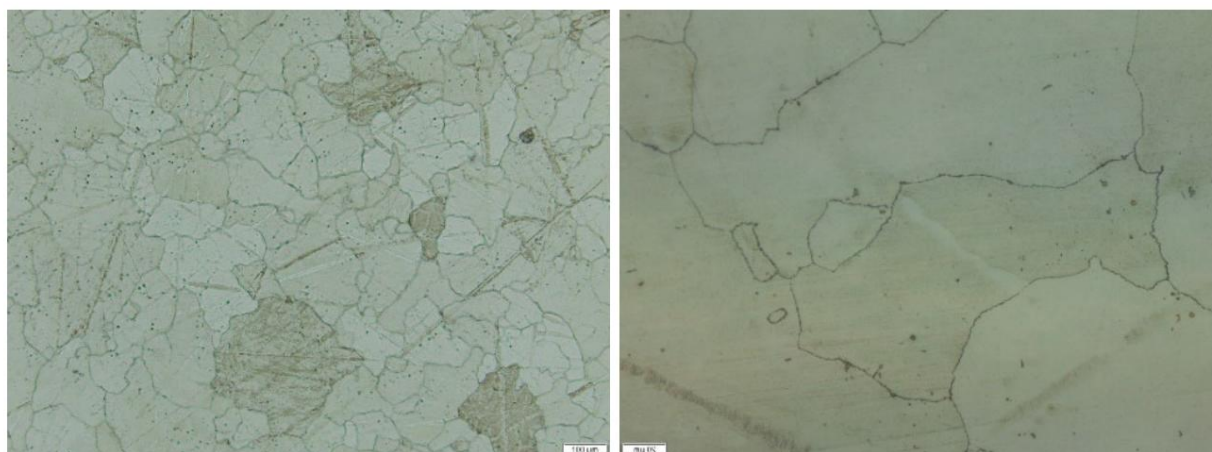
a)   b)

Fig. 4.4 *Optical microscopy images of sample P1, Marble attack, a)M=100x; b) M=500x;* In the case of sample
P1, the solidification structure shows a fairly high homogeneity, which

indicates that during cooling the degree of undercooling ÿTr had corresponding values for

the unfolding of the diffusion phenomena specific to this alloy.
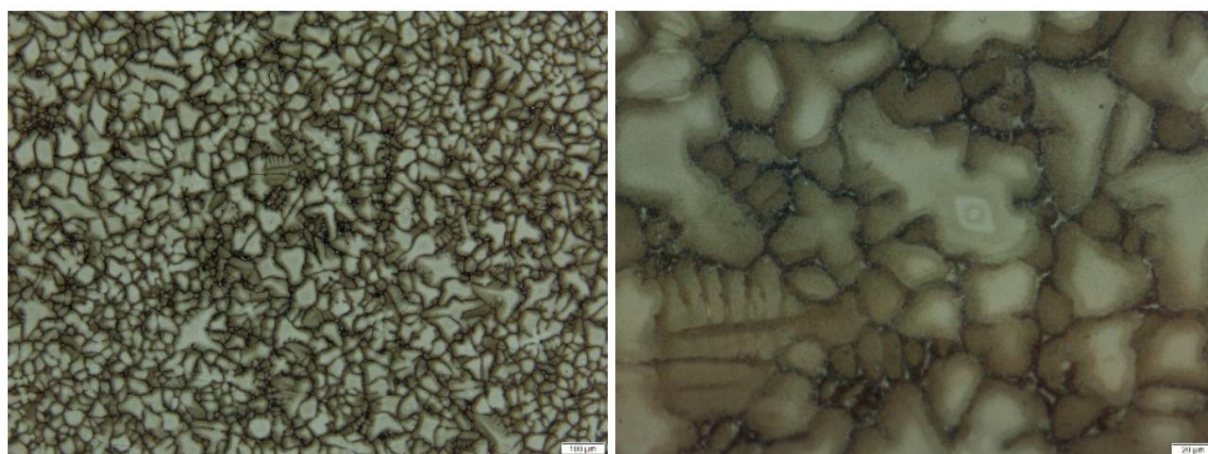
a) b)

Fig. 4.5. *Optical microscopy images of sample P2, Marble attack, a)M=100x; b) M=500x;*
For sample P2, the microstructure images after solidification show a degree of

higher inhomogeneity, a clear indication that the degree of undercooling ÿTr specific to the elaboration process

casting approached was somewhat higher for the chemical composition of this alloy,
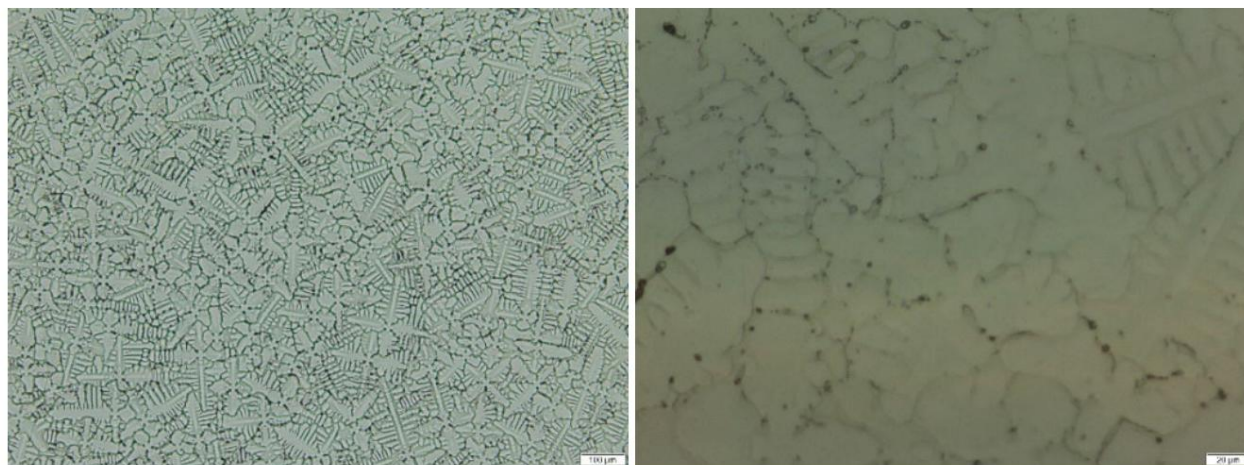
a) b)

Fig. 4.6. *Optical microscopy images of sample P3, Marble attack, a)M=100x; b) M=500x;*
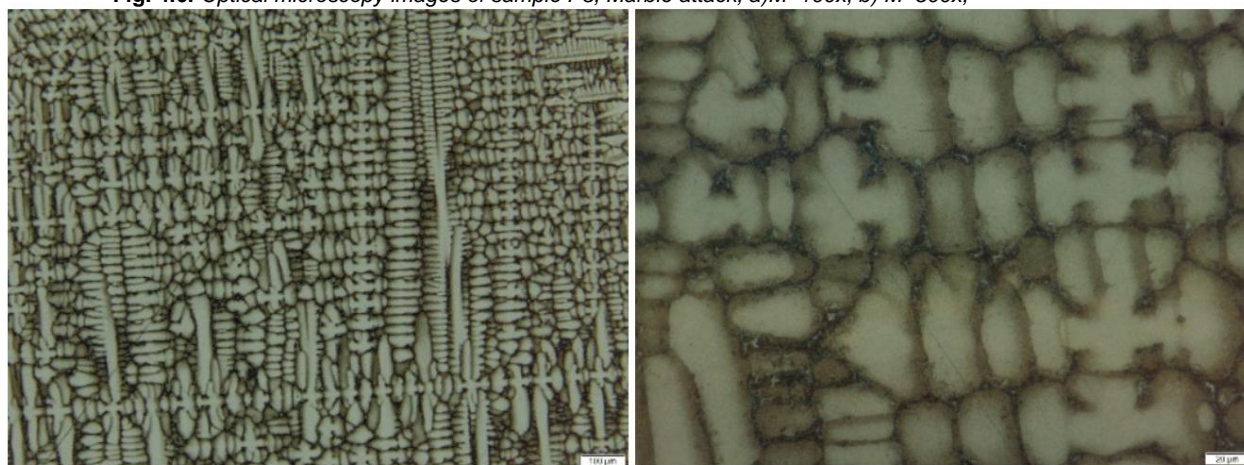
a) b)

Fig. 4.7. *Optical microscopy images of sample P4, Marble attack, a)M=100x; b) M=500x;*

Next, the microscopic analysis for samples P3 and P4 will be carried out in parallel, the samples having many similarities. They have in common the fact that in their chemical composition it increases progressively the proportion of hardly fusible elements (Re, W, Ta). The result is obtaining structures with high chemical and structural inhomogeneity, represented by the massive occurrence of formations dendritic.
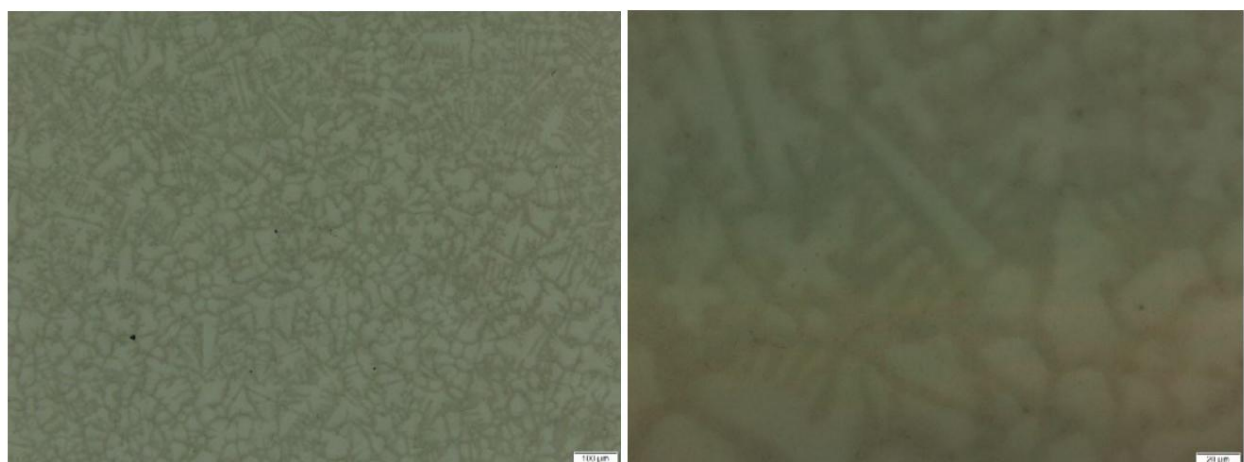
a) b)

Fig. 4.8. *Optical microscopy images of sample 5, Marble attack, a)M=100x; b) M=500x;*

Sample P5, with the newly proposed, more economical chemical composition, brings a more distinctive structure after solidification. In a way, it can be likened to P2, in the sense that the degree of homogeneity is higher, without excluding dendritic formations here either, more clearly visible at higher magnification powers. As a particularity, a finer granulation is noticed, compared to the other investigated evidence.

4.4.2 Structural and compositional analysis by scanning electron microscopy (SEM) associated with characteristic X-ray energy spectroscopy (EDS)

More in-depth information on the structure and local chemical composition of the samples experimentally obtained after elaboration can be obtained by scanning electron microscopy associated with characteristic X-ray energy dispersive spectroscopy (EDS).
Figure 4.9 shows the electron microscopy of sample P1.

(a)   (b)
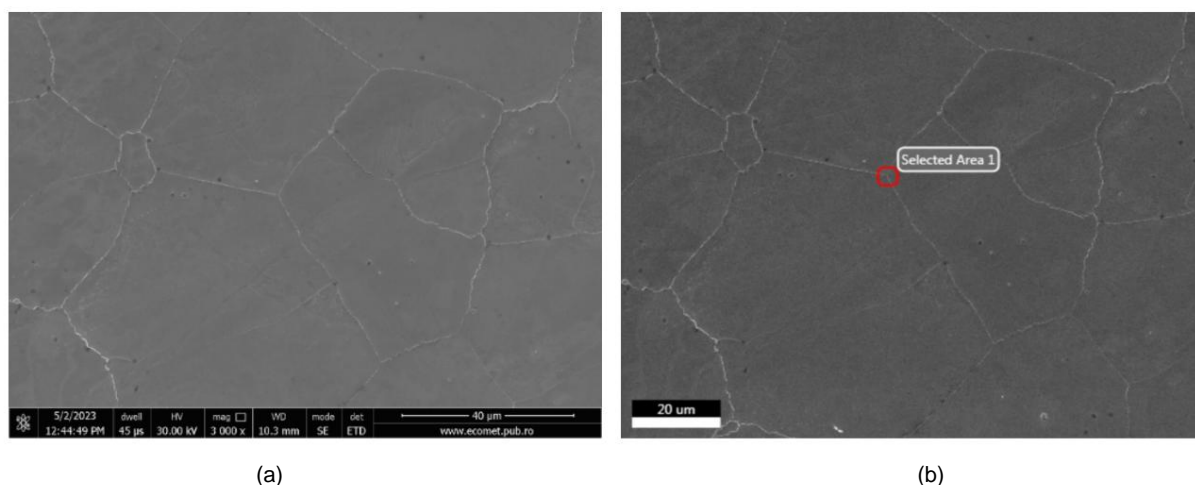
Fig. 4.9. *Scanning electron microscopy (SEM) images of sample P1*
a)   Image of secondary electrons M=3000x
b)   Backscattered electron image specifying the area where the analysis was performed
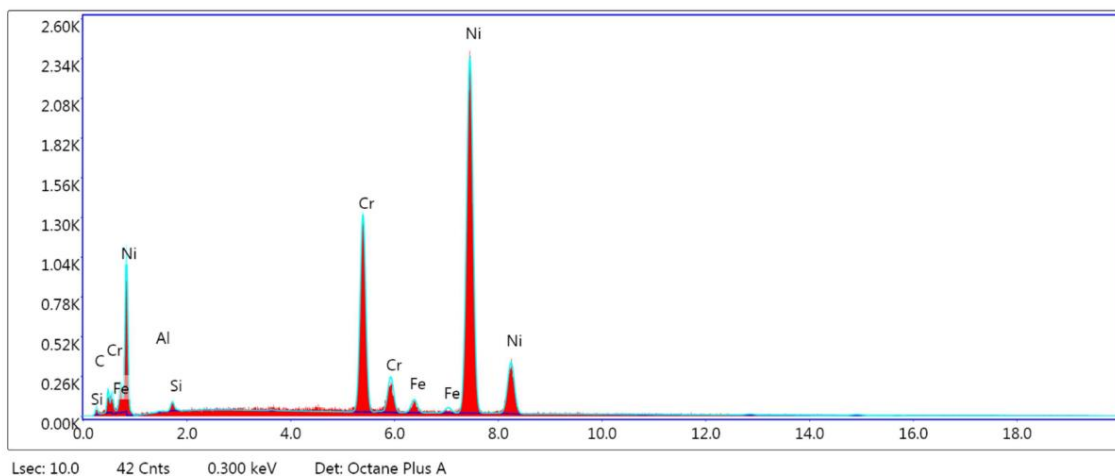*compositional EDX*

Fig. 4.9c. *Energy dispersive X-ray spectrum of sample P1, for the microarea analyzed in the figure*

4.9.b

Secondary electron SEM image (a) reveals a granular structure, similar to crea

observed by optical microscopy and belonging to the solid solution ÿ. At the same time the grain boundaries

shows thickened areas which morphologically belong to the ÿ' (Ni3Cr) phase.

Spot chemical analysis in the "selected area" located in the axial zone of a dendrite

sol.sol.ÿ (tab. 4.6) highlights, among other things, an important amount of Re, which confirms the hypothesis

[113], [115] that this element tends to concentrate in the intradendritic zone. Latest

electron microscopy information refers to sample P5 (fig. 4.13).

(a) (b)
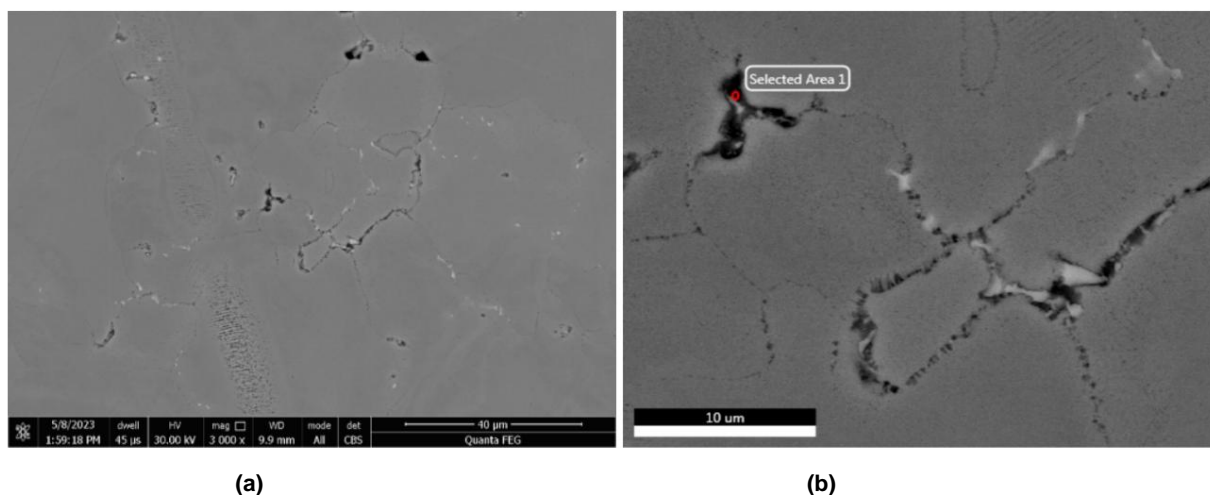
Fig. 4.13. Scanning electron microscopy (SEM) images of sample P5
a) Image of secondary electrons M=3000x
b) Image of radioscattered electrons with the specification of the area where the EDX compositional analysis was performed
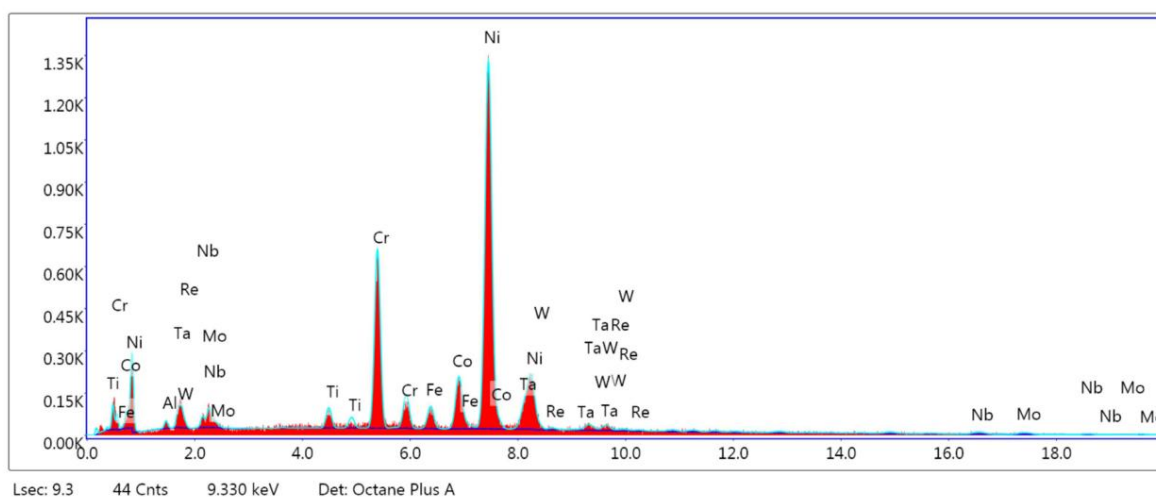
Fig. 4.13c *Energy-dispersive X-ray spectrum of sample P5, for the microarea analyzed in figure 4.13.b*

The dendritic aspect of the P5 sample narrows as the elemental composition decreases

hard to fuse. It still persists, as was also noted in optical microscopy analysis, being

the image of secondary electrons comes more clearly (figure 4.13.a).

As a general conclusion following the structural analysis performed by optical microscopy and

electron microscopy, it turns out that all experimental samples have a lower or higher degree

of structural inhomogeneity resulting from solidification. So that they are suitable for testing

what will follow, it becomes absolutely necessary to be homogeneous, so that the next step in the process will be represented by the application of HOMOGENIZATION ANNEALING.

4.5. Homogenization of elaborated alloys; Homogenization annealing

4.5.1 Purpose of homogenization annealing. The proposed thermal regime

Homogenization annealing aims at the advanced removal of inhomogeneous structures, dendritic, obtained after solidification, bringing the metallic material to a state of structural equilibrium and of tensions.

The heat treatment was applied in a "chamber-type" laboratory furnace, existing in the laboratory of the ECOMET center, electrically heated with electric resistances, having a maximum temperature T = 1400 °C.

Figure 4.14 shows the image of the furnace

***Fig. 4.14.** Electric heat treatment furnace used for homogenization annealing*

The 5 samples were placed individually on the hearth of the furnace, spaced between them, so that heat flow to produce uniform heating. The heating speed as well as the cooling speed have been set at Vrac= Vrac= 5 °C/min.

Figure 4.15 shows the thermal regime of homogenization annealing, applied simultaneously to the 5 samples.
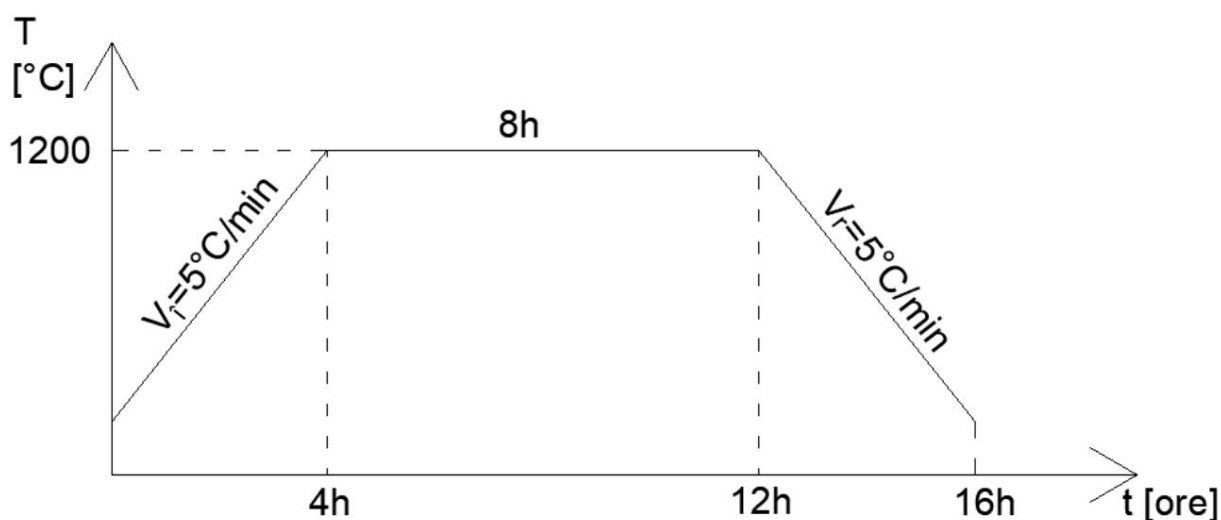
Fig. 4.15. Thermal regime during homogenization annealing

4.5.2. Hardness tests on homogenized alloys

The hardness tests were carried out at a load of 2kgf, the results being presented in table 4.3 where the values for each individual test as well as the average hardness value are found after 5 measurements.

The results of the hardness tests after the elaboration and heat treatments of the alloys, is presented in fig. 4.18.
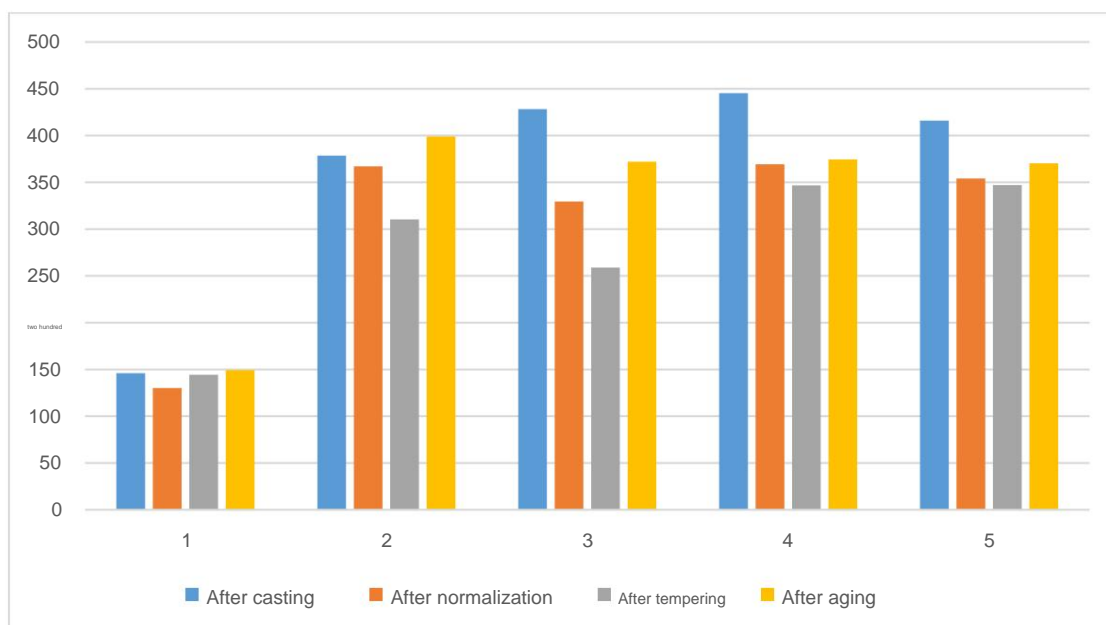
Fig. 4.18. Graphical representation of alloy hardness values after processing, homogenization, solution quenching and artificial aging

Analyzing the hardness values for the five samples after aging, it is found a decrease in its value for samples P3, P4 and P5, an increase for P2 and a maintenance of hardness for P1, compared to the values obtained after casting.

4.5.3 Structural analysis by metallography of samples after homogenization annealing

4.5.3.1 Structural analysis by optical microscopy

After the usual protocol of metallographic preparation and attack with Marble reagent, the 5 samples annealed were studied only at the magnification power M=100x, the images being considered conclusive for observing new structural details.

In fig. 4.19 shows the microscopy of sample P1 after homogenization.

Fig. 4.19. *Optical microscopy image of sample 1 – homogenized. Marble Attack (M = 100x (a);*

The image brings to the fore a granular sol.sol.ÿ structure that is not very different from

optical microscopy image of sample P1 as cast. Granulation appears slightly increased, as a result of

high temperature and prolonged holding time. Specific links are also visualized

of the CFC crystallization system, that of sol.sol.ÿ, the grain boundary, in small quantity, can be observed

and in the ÿ' phase in the form of darker, brown areas).

As in the case of optical microscopy analysis of cast samples, in this case also the samples

homogenized P3 and P4 will be studied simultaneously due to their compositional and structural proximity.

Fig. 4.21. *Optical microscopy images of sample 3 – homogenized. Marble Attack (M = 100x (a);*
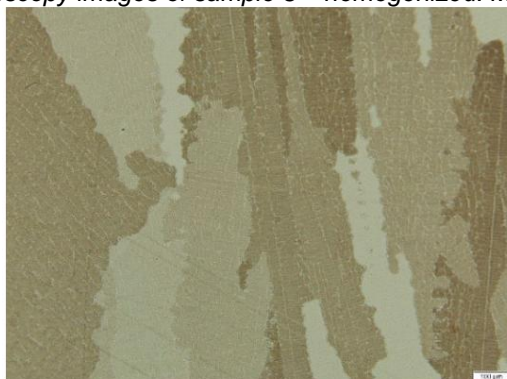
Fig. 4.22. *Optical microscopy images of sample 4 – homogenized. Marble Attack (M = 100x (a);*

Both sample P3 and sample P4 maintain the oriented character that was in the homogenized state

already signaled after casting. Homogenization annealing is not phase-transformed, so it will not

had the ability to radically alter all structural details.

The last optical microscopy image in this analysis group is reserved for the homogenized P5 sample. In fig. 4.23 its microscopy is shown.

Fig. 4.23. *Optical microscopy images of sample 5 – homogenized. Marble Attack (M = 100x (a);*

4.5.3.2 Structural and compositional analysis by scanning electron microscopy (SEM) coupled with characteristic X-ray energy dispersive spectroscopy (EDS)

Electron microscopy will be applied as an analysis method to detail the information structural obtained by optical microscopy, and point chemical analysis will be able to identify more precisely (even to elucidate) the nature of crystalline particles to allow a complete analysis of structures after homogenization annealing.

The analysis will begin with the study of sample 1, homogenized, and the specific images are inserted in fig. 4.24.
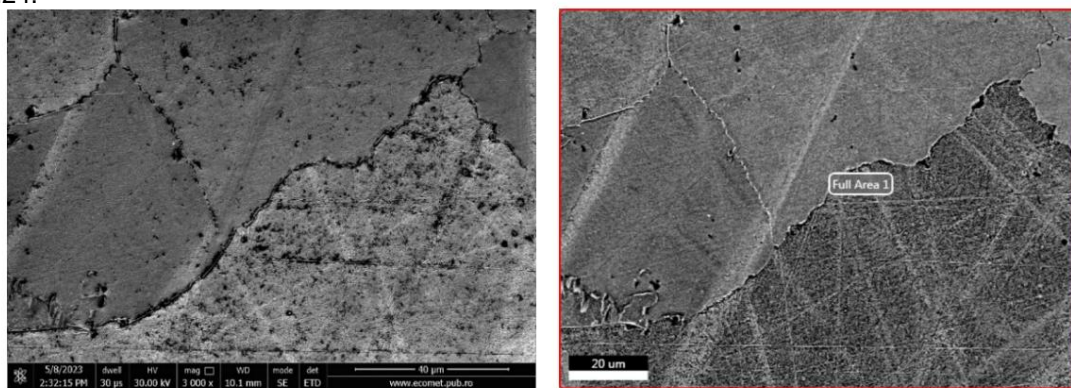
a.   b.

Fig. 4.24. *Scanning electron microscopy (SEM) images of P1-homogenized sample*
Image of secondary electrons M=3000x
Backscattered electron image specifying the area where the analysis was performed
a) b) compositional EDX

Fig. 4.24. c. *The energy dispersive X-ray spectrum of sample P1, for the microarea analyzed in figure 4.24.b - homogenized*

Both the secondary electron image and the backscattered electron image (de composition) shows a reduced structure, effect of homogenization annealing.

The grain boundary, tinted differently from the rest of the image (bright in the composite image) signals the existence of a new phase. Recorded spot chemical analysis in just such microzone (tab. 4.10), from the analysis of the result, a concentration of Ni and Cr values can be noticed. If the atomic concentration ratio is performed $\frac{\%}{\%} = \frac{70.79}{24.08} = 2.93 \sim 3$, which leads to

identification of the Ni3Cr compound, therefore the ÿ phase.

The electron microscopy images specific to sample 2 are inserted in fig. 4.25

A

b

c

25
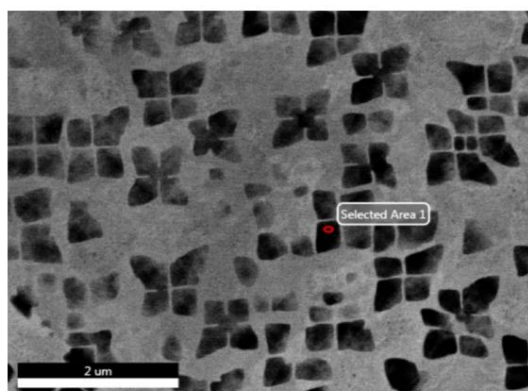
Fig. 4.25. Scanning electron microscopy (SEM) images of P2-homogenized sample
a) Image of secondary electrons M=3000x
b), c) Image of radioscattered electrons with the specification of the area where the analysis was performed
   compositional EDX (M=12000x);
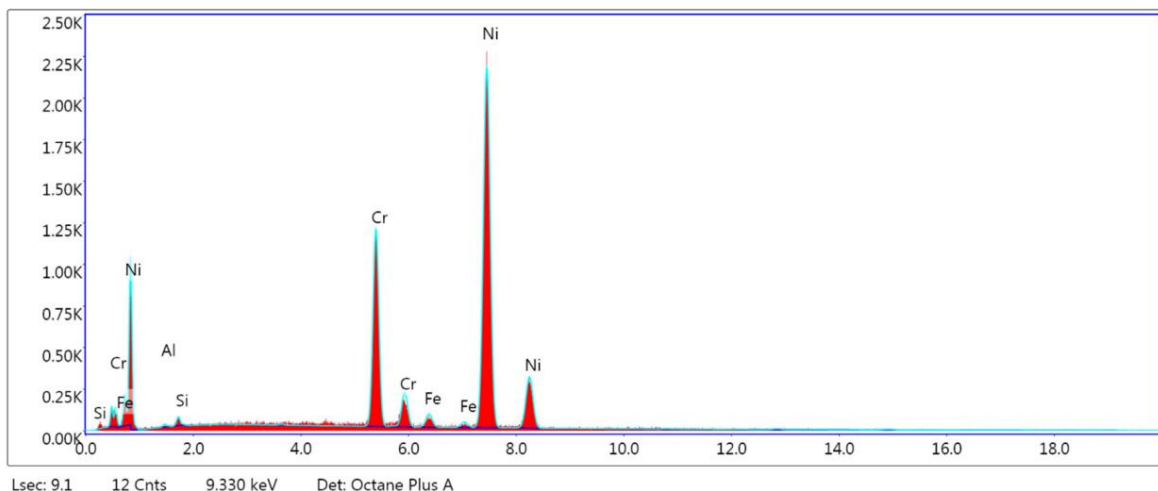

Lsec: 9.2   113 Cnts   2.320 keV   Det: Octane Plus A
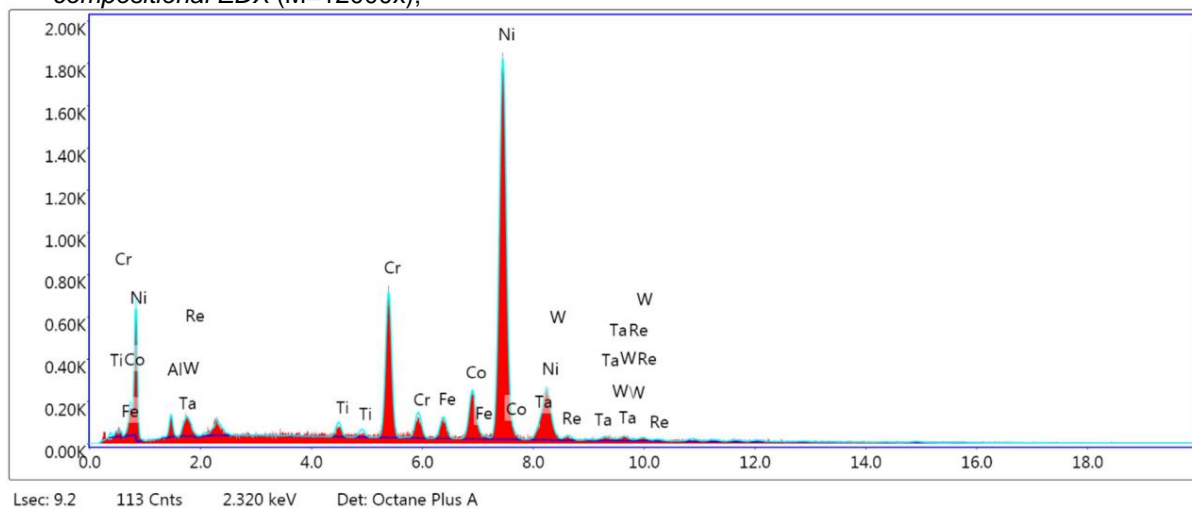
Fig. 4.25.d. Energy dispersive X-ray spectrum of sample P2, for the microarea analyzed in figure 4.25.c - homogenized

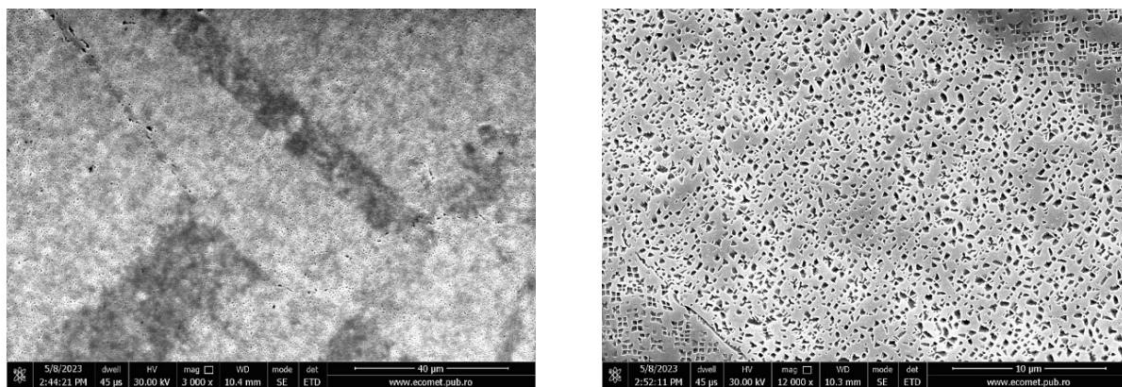The secondary electron image shows a specific granular structure

of the solid solution ÿ, noting also in the electron microscopy the coarse granulation. The image of

backscattered electrons, more sensitive to composition, brings more in-depth details.

More in-depth structural information is obtained by studying the composition image of homogenized

sample 4, recorded in the microregion of fig 4.27e. Figure 4.27f shows the spectrum of

X-rays resulting from chemical analysis in the selected area, and the values are inserted in table 4.14

compositional.
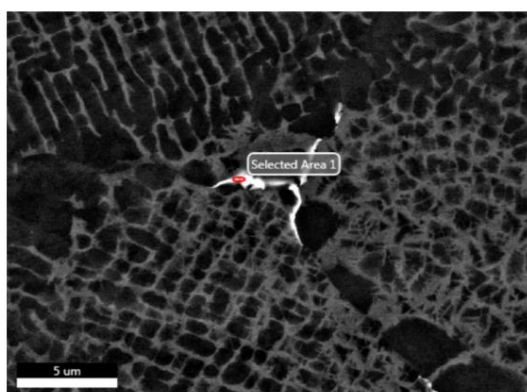
Fig. 4.27e. – Image of backscattered electrons (composite image) in another area of the sample 4 -

Attention was focused on the particle of increased brightness and with filiform morphology

– contorted, identified in previous micrographs as the LAVES phase (formula AB2 or

A2B). The results of point chemical analysis even facilitate the identification of the chemical composition

(tables 4.14). They meet the conditions of the LAVES phases [17], the metals:

Co - rCo =1.26 A°

Ta – rTa =1.70 A°

26

W – rW =1.62 A°

where r = atomic radius, A° (Goldschmidt radius)

$$\frac{+}{rCo} = \frac{1.62 + 1.70}{1.26} = \sim 1.31 \ddot{y} \; 1.225$$

Obs: The condition for a LAVES phase to form [17] is ca $\dfrac{}{rB} \sim 1.225$

- Regarding Ta and W, the average atomic radius was considered, without making a very calculation strictly regarding the participation of each element in the chemical composition.

Therefore, the analyzed LAVES phase can be considered (table 4.15) with the following components:

$$\frac{\%}{\% \, (+)} = \frac{12,17}{1.34+4.26} = 2.17 \sim 2$$

In conclusion, the LAVES phase, which is a topologically defined compound [17], can have the formula chemical **Co2 (Ta,W).**

The cycle of SEM electron microscopy investigations regarding the experimental samples in the homogenized state ends with sample 5. In fig. 4.28 the SEM electron microscopes are inserted own sample 5.

A

b

c.

Fig. 4.28. *Scanning electron microscopy (SEM) images of P5-homogenized sample*
a) Image of secondary electrons M=3000x;
b), c) Image of radio-broadcast electrons specifying the area where the EDX compositional analysis was performed – M=12000x;

4.6. ConCluSIonS

- The development of INCONEL alloys in a vacuum and argon atmosphere, allowed the melt to be

    protected during their development and ingot casting.

- The alloying elements present in the chemical composition of the developed INCONEL alloys
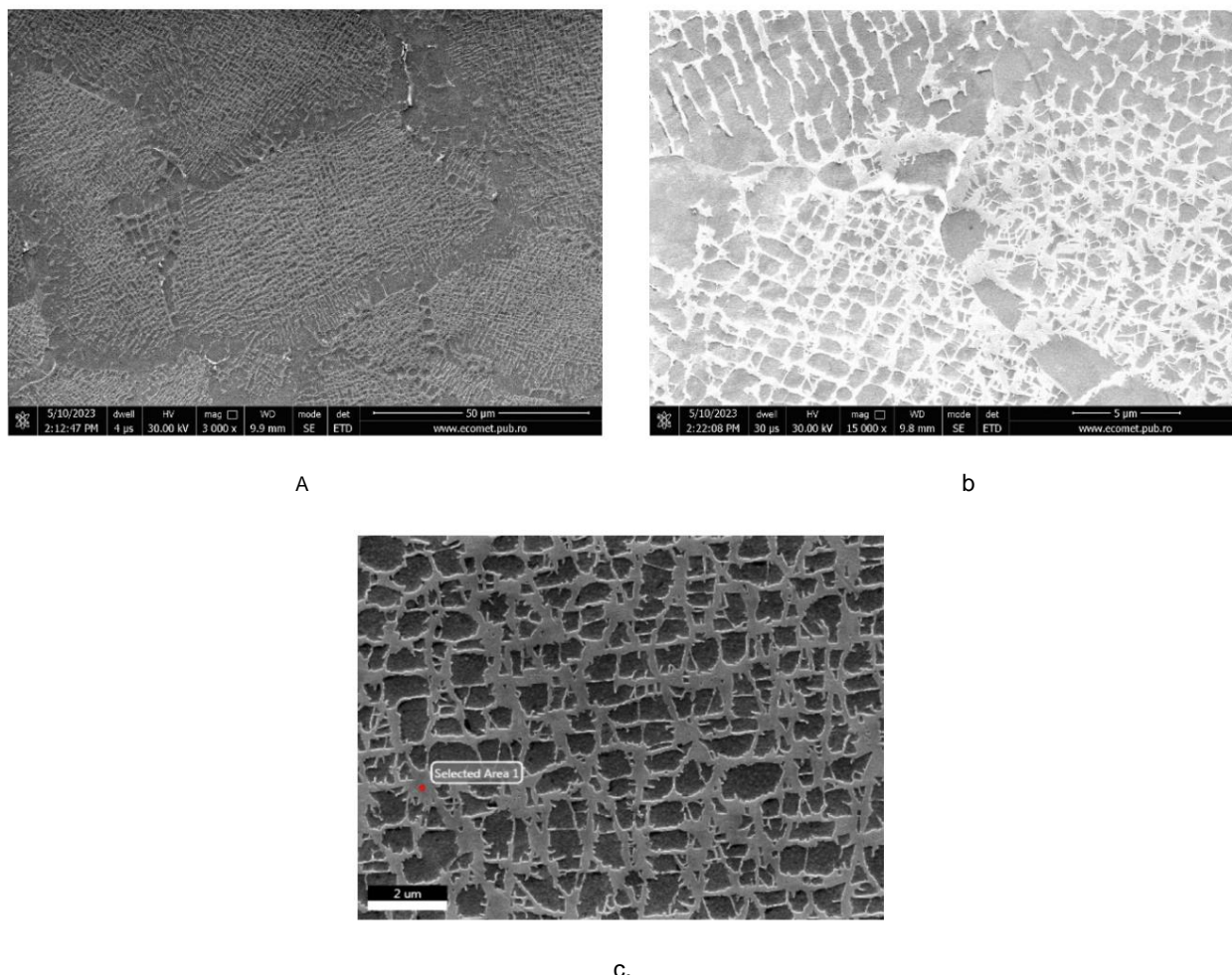
    (Ta, W, Re) are hardly fusible elements, with very high melting point values

    high, which globally permutes the melting temperature of the alloy to higher values. Under

    these conditions, the degree of subcooling ÿTr specific to the process becomes higher, and

    the implications are negative on diffusion phenomena, which take place more slowly, and

    the structure begins to have an inhomogeneous character.

- Structural analysis performed by optical microscopy and electron microscopy, results

    that all experimental samples have a greater or lesser degree of inhomogeneity

    structure resulting from solidification.

Chapter 5. MODIFICATION OF THE STRUCTURE AND PROPERTIES OF ALLOYS EXPERIMENTAL THROUGH THERMAL TREATMENTS

5.1. Thermal treatments applied. Proposed working regimes

Thermal treatments represent a very widespread alternative to modify the structure, and therefore also the properties of metallic materials. The essential condition is that they present phase transformations in the solid state, otherwise heat treatments are ineffective.

5.1.1. Tempering for solution; Parameters of the working regime

Solution quenching is the type of quenching that aims to solubilize the phase

secondary. To make this possible, the alloy must be heated in the range of homogeneity

(above the "SOLVUS" curve) at a temperature that should not exceed the temperature by much

solvus: TT=Tsv+10÷15°C.

Then there is a holding stage for the complete solubilization of the secondary phases, followed by a

rapid cooling. Rapid cooling is usually done in water, the most common cooling medium

encountered, which by the rapidity with which the metallic material is brought to the temperature

environment cancels diffusive phenomena.

5.1.2. Artificial aging; Parameters of the working regime

Aging is the heat treatment applied after solution quenching and has

as the objective to bring the hardened metal material to a state closer to the structural balance,

with the aim of obtaining high mechanical performances.

The structural phenomena that occur during aging are based on transformations in solid state relating to "Heating Decomposition of Supersaturated Solid Solutions". It follows that all phenomena are produced by diffusion phenomena, bringing the metallic material closer to a state of thermodynamic balance, which will lead to obtaining a controlled structure, which will ensure the mechanical performances pursued.

As a result, a two-stage aging will be applied, at T=720 ⁰C and at T=620 ⁰C. It will be called STAGED AGING, terminologically proposed by the authors of the paper [130], which we adopt

TT = 720 ⁰C; 620 ⁰C

5.1.3. The proposed termination regimes

Figure 5.1 shows the mixed thermal regime for quenching and tempering staged aging
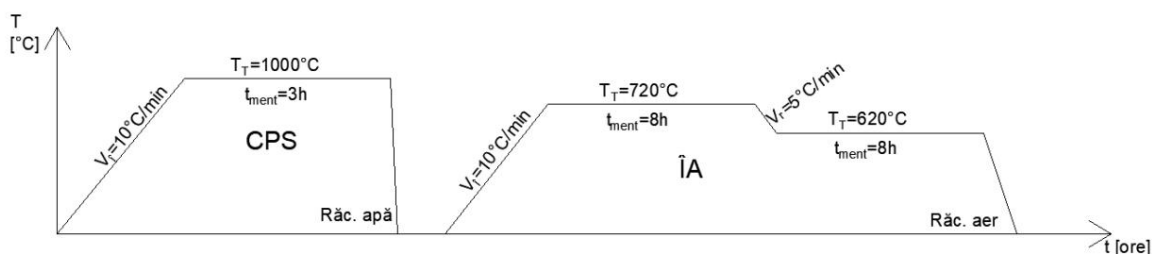
Fig. 5.1. *The mixed thermal regime of CPS + ÎA*

5.3. Analysis by metallography of the experimental samples after the application of quenching for solution

5.3.1. Structural analysis by optical microscopy

In figure 5.3. the optical microscopy of sample 1 is shown.

Fig. 5.3. *Optical microscopy images of sample 1 – solution quality. Marble Attack (M = 100x);*

As with the homogenized structure, sample 4 resembles sample 3. The same is observed oriented structure, with a slightly increased grain size compared to the homogenized one. Not even in this one case no precipitated secondary phases are observed, so the analyzed structure can be named soil.soil.ÿsupersaturated.

The optical microscopy studies end with the analysis of sample 5, shown in fig. 5.7.

Fig. 5.7. *Optical microscopy images of sample 5 – solution quality. Marble Attack (M = 100x);*

CONCLUSION - According to optical microscopy studies in the case of the 5 samples experimental INCONEL structures are obtained sol.sol.ÿsupersaturated, assigned sol.sol.ÿ(supersaturated). Only electron microscopy studies will be able to provide complete information.

5.3.2. Structural and compositional analysis by scanning electron microscopy (SEM) coupled with characteristic X-ray energy dispersive spectroscopy (EDS)

The first sample analyzed by electron microscopy techniques is sample 1, qualified for placing in solution (CPS), the obtained images being shown in fig. 5.8.

| A | b |

Fig. 5.8. *Scanning electron microscopy (SEM) image of sample P1 – CPS*

a. image of secondary electrons

b. backscattered electron image (composite image) specifying the area where it was performed EDS compositional analysis

Fig. 5.8. c. *Energy dispersive X-ray spectrum for the analyzed microarea of sample 1 - CPS*

Table 5.2. *Local chemical composition in the selected area of sample P1 - CPS*

Both secondary electron and backscattered (composite) electron imaging highlights a granular structure, which belongs to sol.sol.ÿ, in this case supersaturated (there is no criterion to distinguish the equilibrium solid solution from the supersaturated one). At the grain limit se observe a light, discontinuous network specific to the secondary phases.

Spot chemical analysis performed on this very network (Table 5.3) suggests that it would phase ÿ' (Ni3Cr). Data processing, with atomic ratio calculation for Ni and Cr, demonstrates that:

$$\frac{\%}{\%} = \frac{65.04}{29.88} = 2.17$$

The latest scanning electron microscopy studies are for sample P5 quenched for solution. The corresponding electron micrographs are grouped in Figures 5.12.
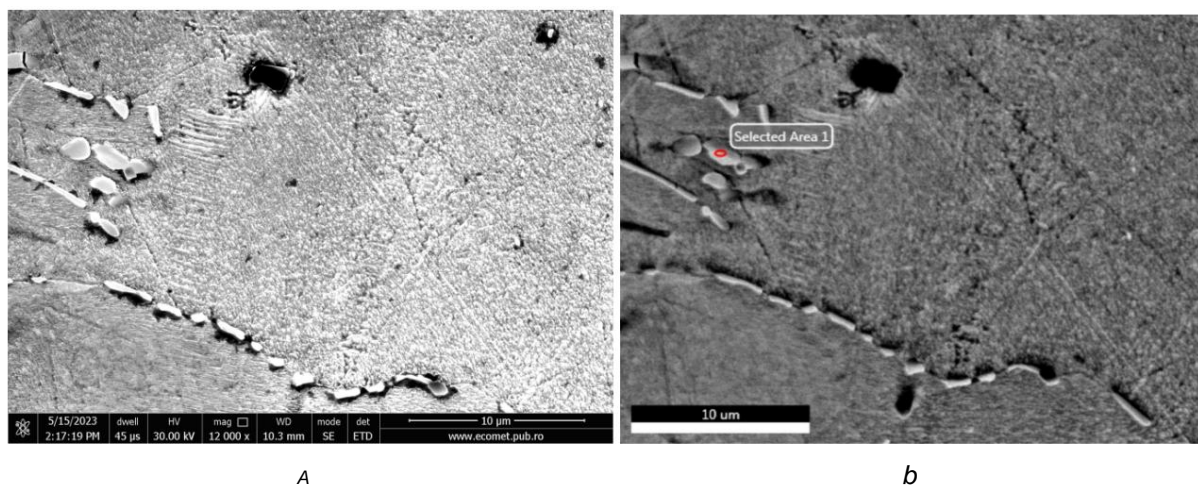

A	b

Fig. 5.12. *Scanning electron microscopy (SEM) image of sample P5 – CPS*

a. image of secondary electrons

b. backscattered electron image (composition image) specifying the area where the EDS compositional analysis was performed
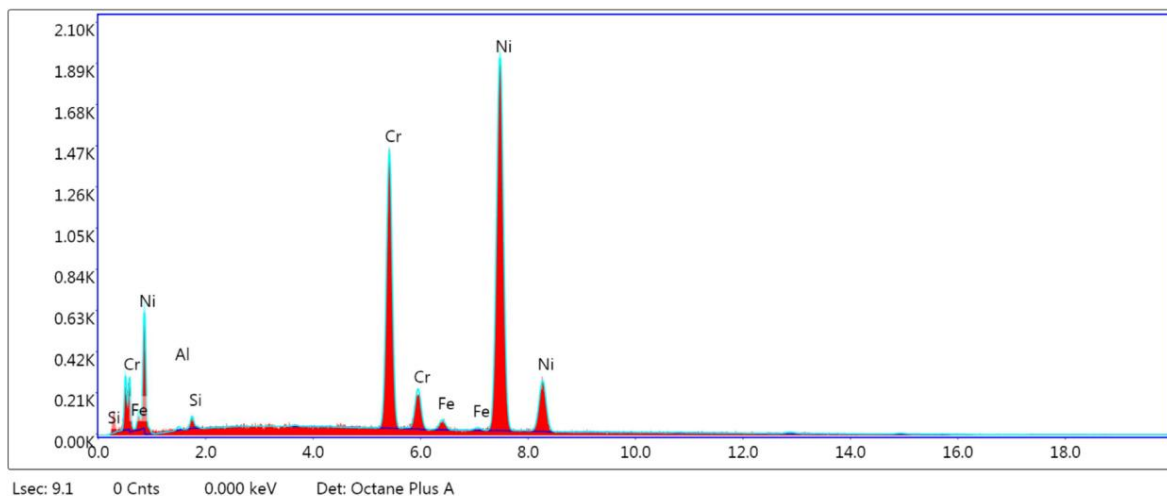
Fig. 5.12. c. *Energy dispersive X-ray spectrum for the analyzed microarea of sample 5 – CPS*

Secondary electron and backscattered electron images capture biphasic structures consisting of sol.sol.ÿ (bright, network-like areas) and ÿ' phase (dark areas).

The micrographs show similarity to those corresponding to the same homogenized sample.

5.5. Metallographic analysis of experimental samples after aging application PARKS

5.5.1 Structural analysis by optical microscopy

In Figures 5.15, 5.16, 5.17, 5.18 and 5.19.

Fig. 5.15. *Optical microscopy images of sample 1 – CPS + Aging. Marble Attack (M = 100x)*
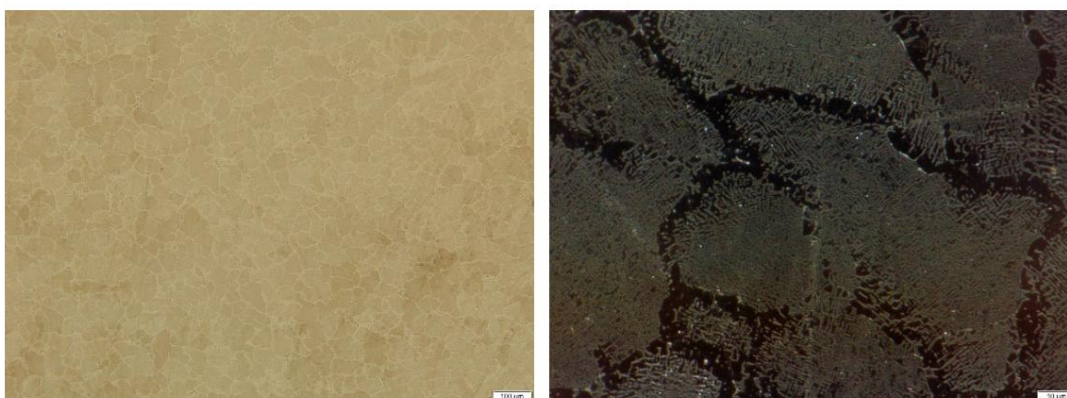
Fig. 5.19. *Optical microscopy images of sample 5 – CPS + Aging. Marble Attack (M = 100x (a);*

1000X (b);

Indeed, the resulting structures after aging are very similar to the resulting ones by solution quenching. As a novelty, a fine dispersion of particles can be noticed in the grains of sol.sol.ÿ visualize, non-existent after tempering. Finely dispersed particles are the result of phenomena of precipitation, specific to aging and the direct result are the hardness increases identified in those 5 samples and denoting that the dispersion hardening mechanism worked.

5.5.2 Structural and compositional analysis by scanning electron microscopy (SEM) coupled with characteristic X-ray energy dispersive spectroscopy (EDS)

The analysis of sample 1 represents the starting point of electron microscopy studies with scans performed on aged samples. The obtained images are reproduced in fig. 5.20.

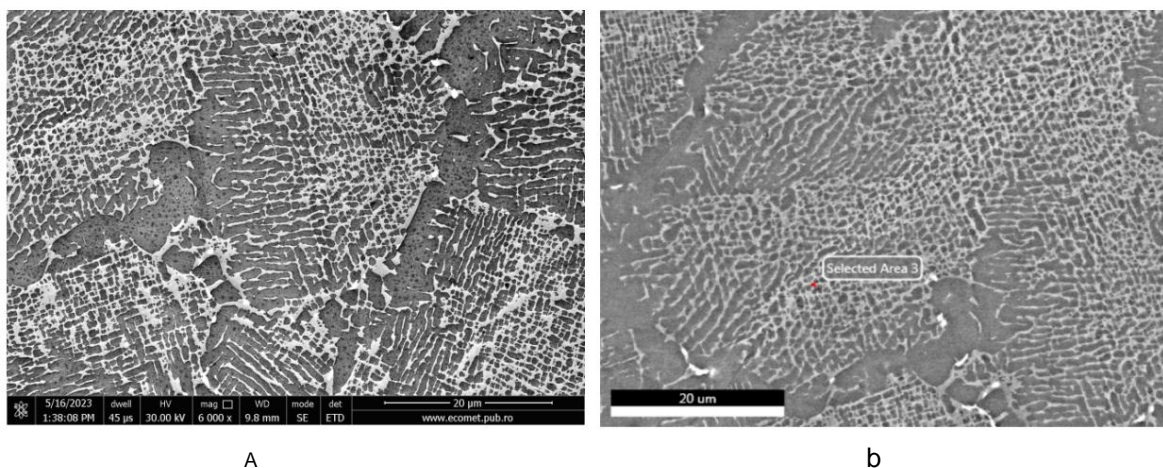A   b
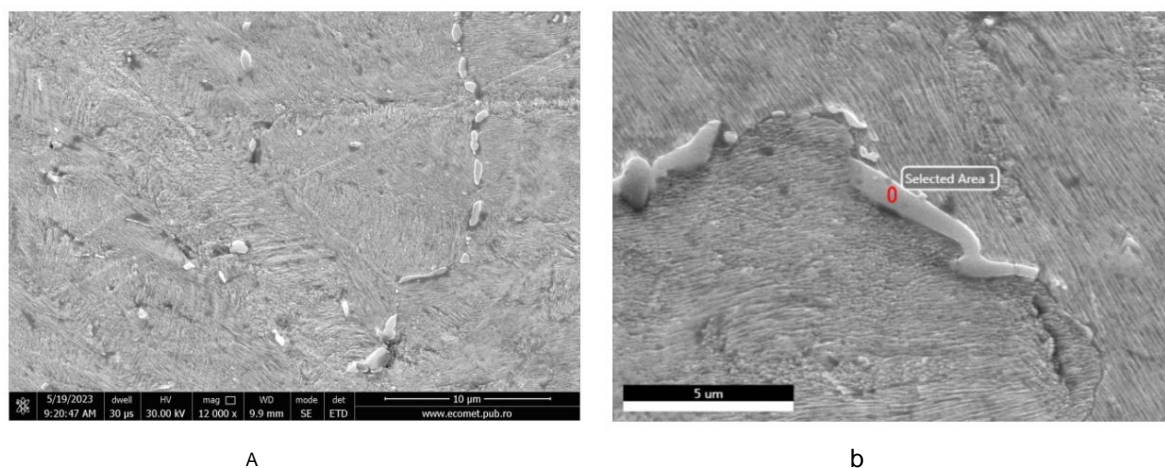
Fig. 5.20. *Scanning electron microscopy (SEM) image of sample P1 – CPS + Pack.*

a. image of secondary electrons
b. backscattered electron image (composite image) specifying the area where the EDS compositional analysis was performed
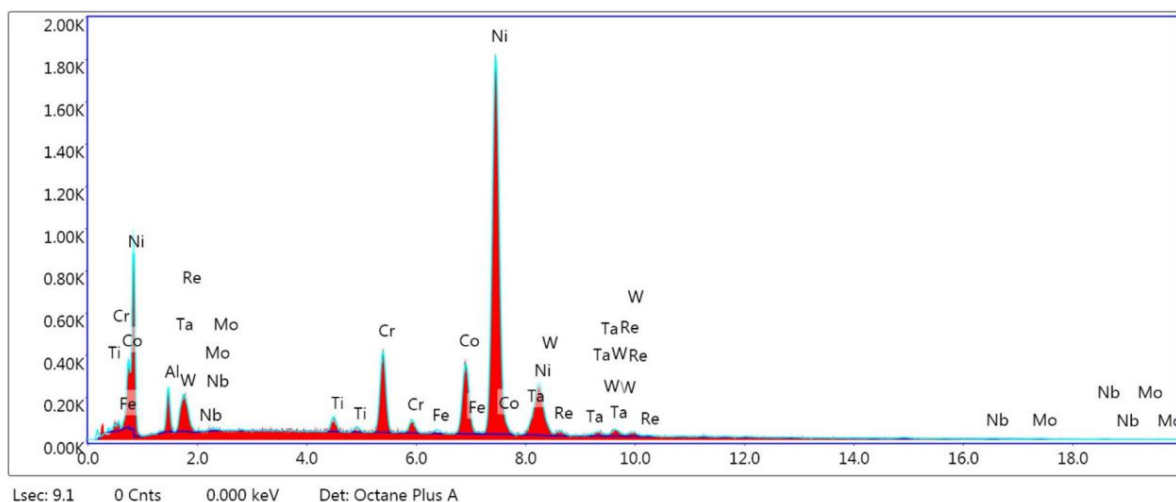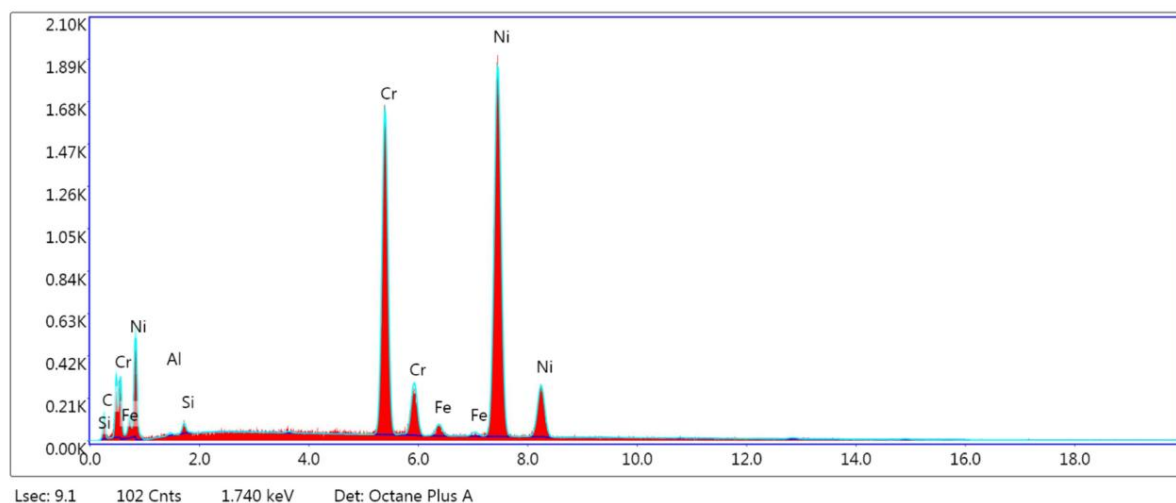

Fig. 5.20.c *Energy dispersive X-ray spectrum for the analyzed microarea of sample 1–CPS + Pack.*

The images provided by electron microscopy highlight a structure in detail granular but also particles anchored in the center of the grain and resulting from precipitation. I'm not very dense, which justifies the rather small increase in hardness after aging.

However, a distribution "in a row" of some luminous particles of shapes is quite clearly visualized regular, visible in the secondary electron image (fig. 5.20a), but also in the composition image (fig. 5.20b).

In conclusion, the structurally identified light network belongs to the Cr23C6 compound.

The latest batch of scanning electron microscopy investigations of alloys aged refers to sample 5, whose micrographs are shown in figure 5.24.
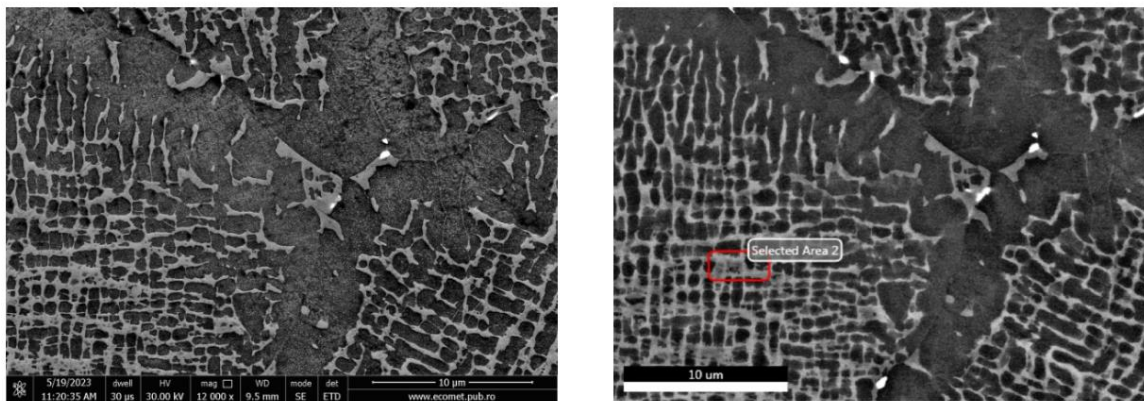
Fig. 5.24. *Scanning electron microscopy (SEM) image of sample P5 – CPS + Pack.*

a. image of secondary electrons
b. backscattered electron image (composite image) specifying the area where the EDS compositional analysis was performed
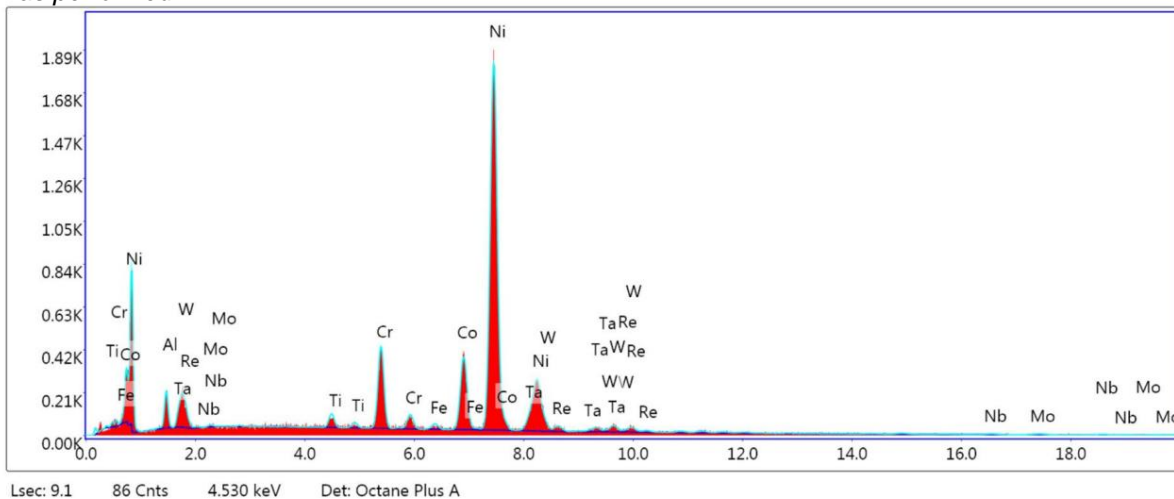
Fig. 5.24. c. Energy dispersive X-ray spectrum for the analyzed microarea of sample 5 – CPS+Pack.
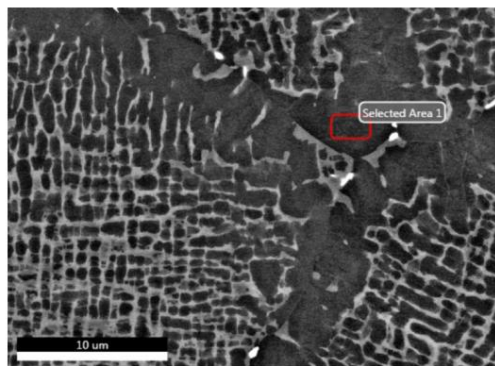
Fig. 5.24.d. *The same backscattered electron image (composite image) in fig. 5.24.b, but with specifying another area where EDS compositional analysis was performed*

5.6. Corrosion behavior of Inconel superalloys

5.6.1. Materials and methods

The following materials were used: 5 Inconel superalloy samples, fig. 5.25, acid solution

sulfuric pa, three-electrode electrochemical cell with platinum counter electrode and reference electrode

Ag/AgCl 3m, potentiostat/galvanostat Reference 300 Gamry.
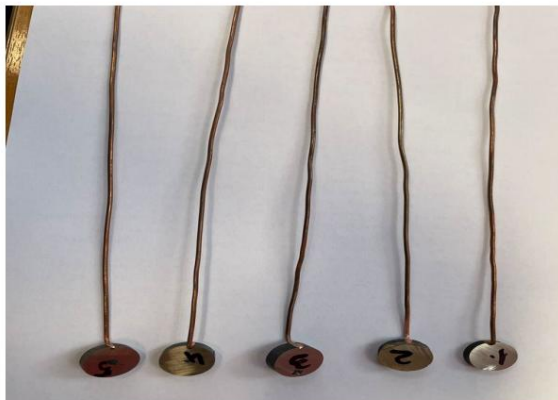
Fig. 5.25. *Inconel samples prepared for corrosion testing*

Evaluation of the corrosion behavior of nickel alloys in 0.1N sulfuric acid solution at

the temperature of 25°C was carried out by the following techniques

5.6.2. result

Because the redox potential of nickel is close to the potential of hydrogen on the scale

redox, nickel does not readily release hydrogen during corrosion in aqueous media without chlorine ions.

The dissolution process is kinetically inhibited because Nickel has the ability to form a film

passive and the presence of an oxidant will strengthen its passivity.
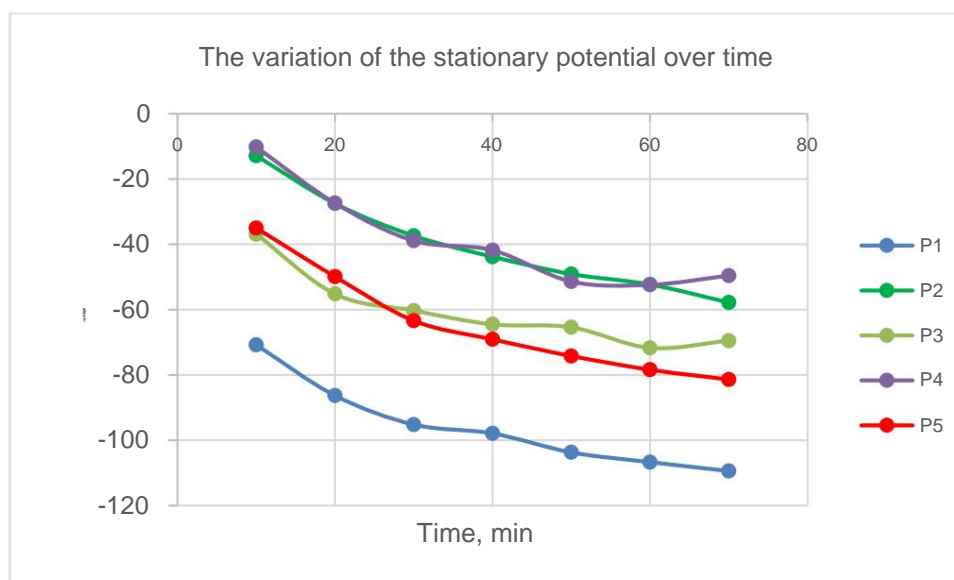
Fig. 5.26. *Variation of stationary potential with time for samples P1–P5*

A similar variation of the stationary potentials of the five alloys is observed, the curves are

relatively parallel. All samples have a normal OCP negation variation due to the dissolution of the native passivity film

formed on the surface, there being no fundamental differences between the materials, the OCPs

falls within the gap of 100mV. However, alloys can be grouped into three categories with practical behavior identical, namely P2-P4, P3-P5 and P1. P4 has the most electropositive potential with obvious tendency of moving towards electropositive values, which means that aluminum has compensated for the decrease the chromium concentration on the passivation capacity of the material.

5.6.4. Anodic polarization

The anodic polarization curves have the classical form of NiCr alloys with the potential domains, according to figure 5.27. The cathodic branch represents the field of hydrogen evolution, and the anodic oxidation domain, active domain, passive and transpassive domain.

The presence of very well highlighted peaks in the P2-P5 alloys can be the proof of the existence of some fine phases individualized of the different alloying elements, and the very broad active peak of sample P1 which includes all these processes a proof of the high homogeneity of the material or some treatments thermal.

1-P1/ 2-P2/ 3-P3/ 4-P4/5-P5
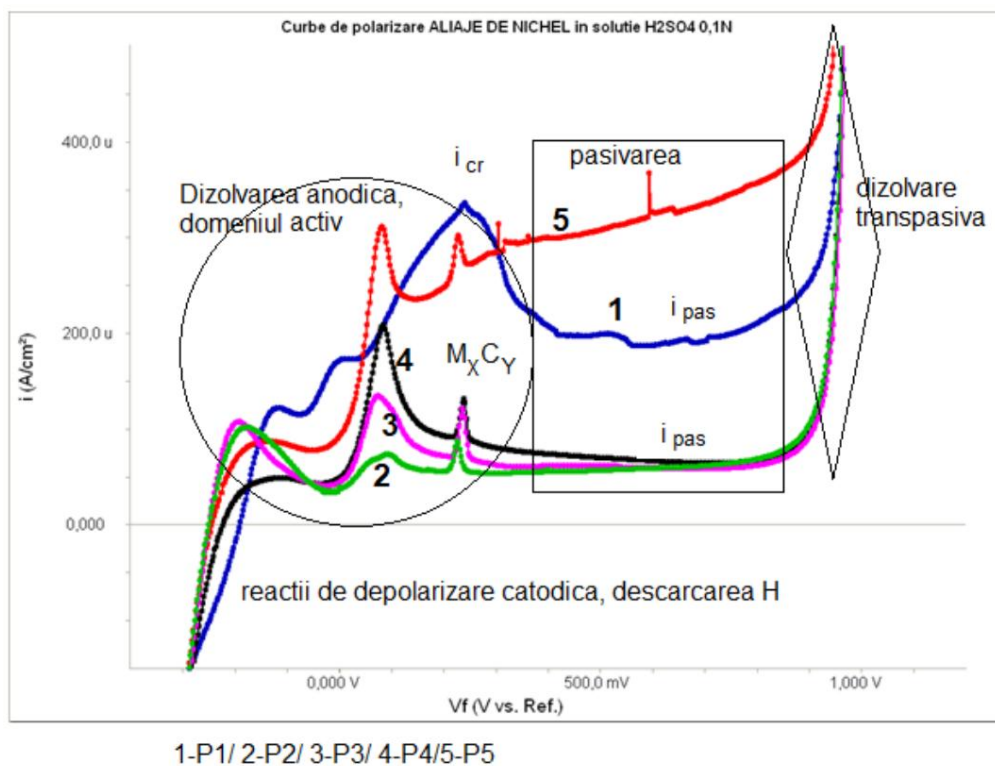
Fig. 5.27. Polarization curves for Inconel P1-P5 superalloys

As a conclusion, P1 and P5 seem to passivate harder compared to the others, but all of them the alloys are passivated, the currents in the passive state are relatively small, between 100 and 350mAcm-2 .

It must be specified that all samples present the same value for the transpassive potential.

5.6.5. The Tafel Slope method for determining the corrosion rate

Tafel curves are shown in figure 5.28. and the values of the corrosion parameters in table 5.13.
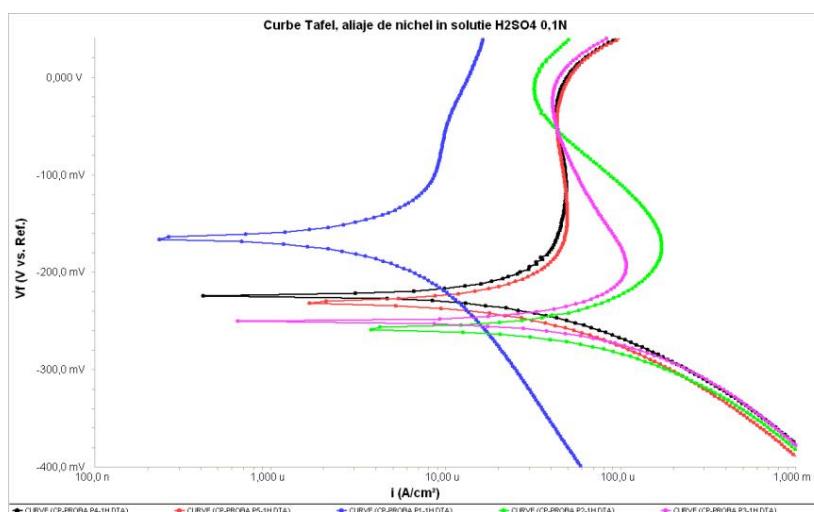
Fig. 5.28. *Tafel curves for determining the corrosion rate of Inconel T1-T5 samples*

From the analysis of the Tafel curves and the corrosion parameters, the following aspects emerge:

- All the curves have very high anodic slopes, which indicates the passivation tendency, a materials;

- The corrosion potentials of the P2-P5 alloys are practically identical with differences of a few tens of mV;

- P4 has the lowest corrosion current density, but very close to P2 and P5.
- P1 has the highest corrosion current density.

Therefore, there are no significant differences between P3-P5 alloys even if the smallest value of the corrosion current density was recorded in the case of the P5 alloy.

5.7. ConCluSIonS

• Modification of the structure and mechanical properties of the INCONEL superalloys proposed for the experiments was possible by applying the mixed heat treatment of SOLUTION TEMPERING and AGING.

• The working parameters (TT and tment) were so chosen that the hardening mechanism se unfolds as efficiently as possible, i.e. through a controlled precipitation of the phases responsible for this effect, taking into account the chemical composition of the alloys but also the specific demands for which INCONELS ARE DEVELOPED.

Head. 6. CASE STUDY - REPORT ON THE DETERMINATION OF THE CAUSES OF FAILURE MULTIPLE SPRINGS IN THE INTAKE AND EXHAUST VALVE SYSTEM MADE OF INCONEL X750 SUPER ALLOY FROM COMPRESSOR DE RECYCLING 122K1

6.1. The objective of the research is to establish the causes that led to the stoppage of a recirculation compressor 122 K1 from a refinery, following the premature failure (5 years) of several springs in the intake and exhaust valve system. Considering the information provided by

specialized literature, it is appreciated that the choice of Inconel X750 superalloy for the execution of springs

of compressors is correct, stating mechanical characteristics in a band

relatively wide, depending on the heat treatment technology, or the degree of cold deformation.

6.2. Macroscopic analysis

6.2.1 Visual examination of springs

29 valve springs were analyzed which were made from wire with a diameter of 0.7

mm, with different appearance - 13 springs, of which 9 whole and 4 broken, are darker in color

(fig.6.1), while other 16 springs, all broken, are light colored (fig.6.2), suggesting conditions of

easier use or shorter usage times compared to more colored springs

dark

Fig. 6.1. Full arch with 10 turns of dark color

Observed under the optical microscope, the ends of the unbroken springs (fig. 6.4a) can be differentiated with

eased by those of the springs that failed in operation (fig. 6.4b).

a)   b)

Fig. 6.4. Spring end in profile: a) spring without break; b) broken spring

6.3. Microfractographic analysis

The analysis was performed on a scanning electron microscope Quanta 450 FEG. They were investigated

the morphologies of arc coils and fracture surfaces, as well as the chemical compositions of some areas

with particular appearance on the surfaces of the springs.

In the first stage, the surface appearance of the wire along the arc turns was analyzed. In figures 6.5

and 6.6 images of the surfaces of dark-looking and colored arcs can be seen, respectively

open, as well as results of chemical composition determinations carried out using the EDS technique.
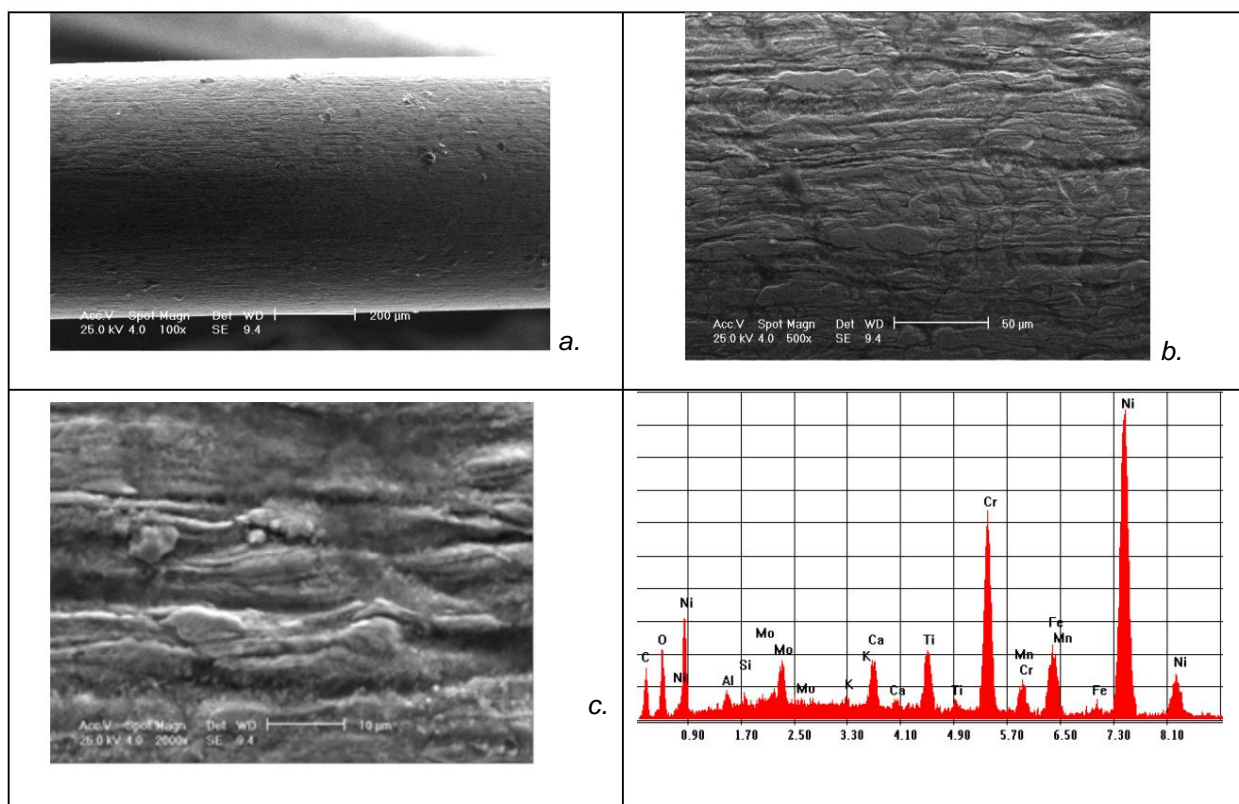
Fig. 6.5. *Secondary electron images of the surface of a dark arc*
[a) ×125; b) ×600; c) ×2000] and qualitative EDS analysis on the spring surface
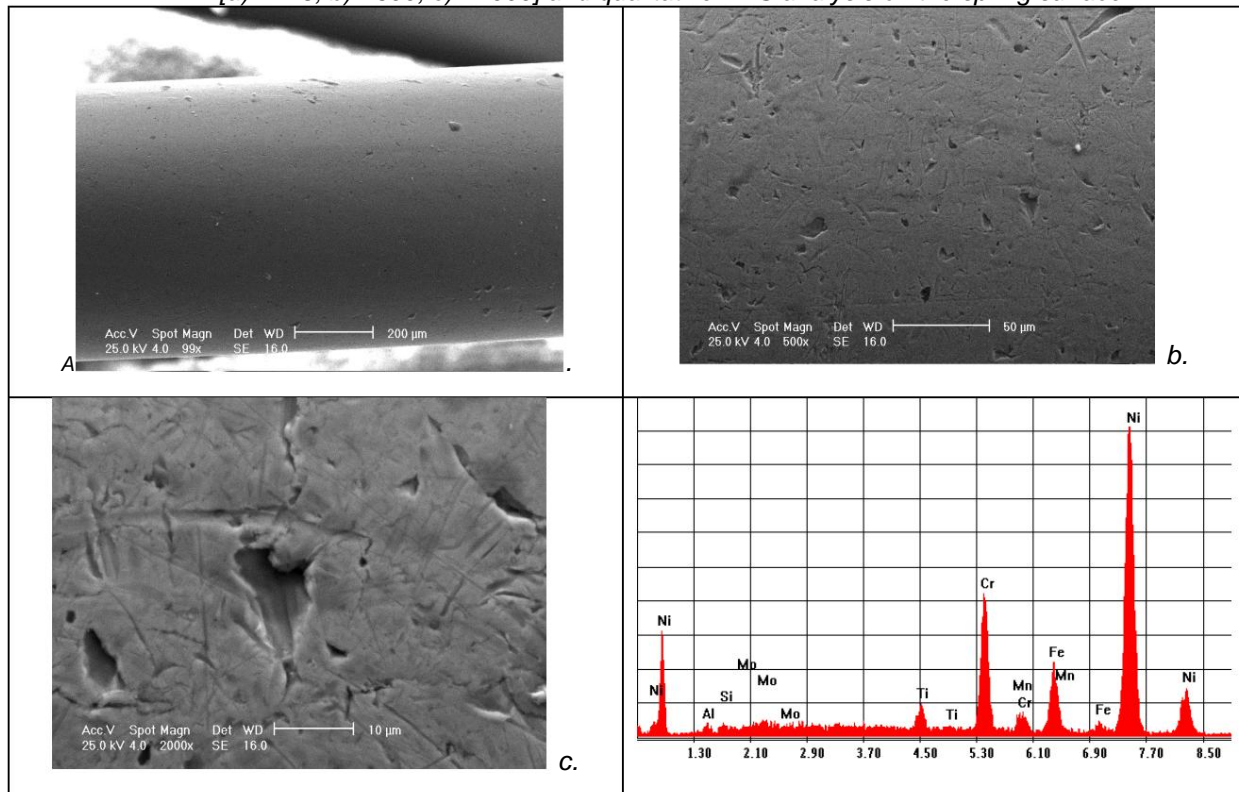
Fig. 6.6 *Secondary electron images of the surface of a light colored arc*
[a) ×125; b) ×600; c) ×2000] and qualitative EDS analysis on the spring surface

6.4. Microstructure and chemical composition

The typical appearance of the microstructure of the material results from fig. 11. Images were obtained on a QUANTA 450 FEG electron microscope.
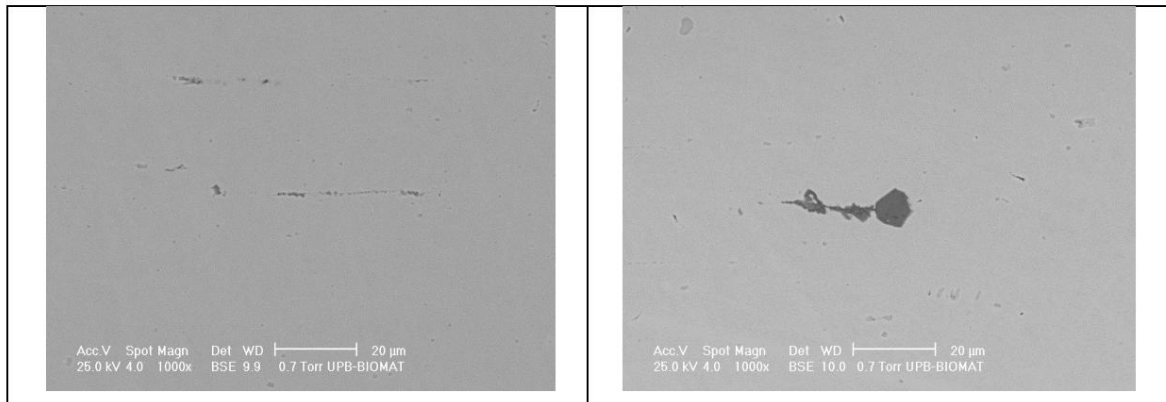
Fig. 6.11. Microstructure of the arc material (NH3/ HCl attack; ×1000)

The microstructure consists of an austenitic metal mass with carbide precipitates

metallic. The nature and chemical compositions of the metallographic compounds were investigated in detail

by the EDS (energy dispersive X-ray spectroscopy) technique.
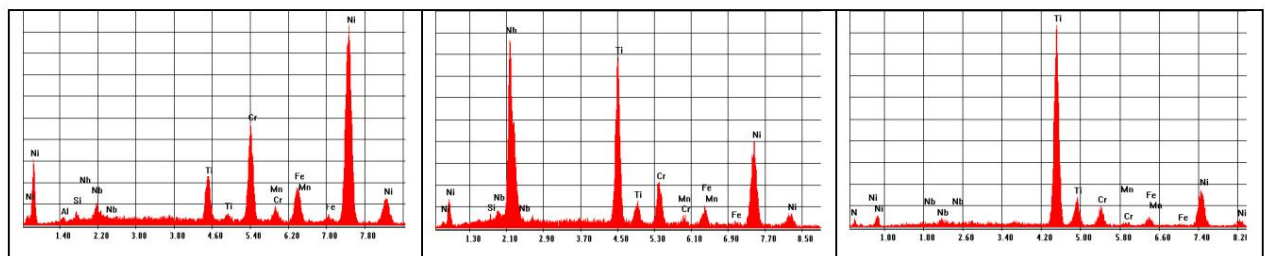
Fig. 6.13. EDS qualitative analysis of the chemical composition of some precipitates present in the microstructure of the spring material

- no significant differences in chemical composition were identified between bows with shades of

different color.

6.6. ConCluSIonS

- The choice of Inconel X750 superalloy for the execution of the valve springs of the compressor

122 K1 is correct, as the corrosion resistance characteristics of this material are known

- The breaks of the springs mainly occurred in the areas of the first three coils at the end of the spring and

resulted from torsional and bending stresses. Predisposing factors for rupture

premature springs were: incorrect geometry in the end zones and possibly excessive resistance

of the wire used to make them.

Chapter 7. GENERAL CONCLUSIONS, ORIGINAL CONTRIBUTIONS AND FUTURE DIRECTIONS FOR RESEARCH

7.1 General Conclusions

Following the theoretical studies and the results of the scientific research carried out, they can be formulated

the following general conclusions:

- Superalloys are metal alloys that resist high temperatures, usually up to 70%

   from the absolute melting temperature.

- Superalloys have excellent creep, corrosion and oxidation resistance as well as good

   surface stability and high fatigue resistance.

- The realization of such advanced alloys allows a higher operating time of

   engines working at high temperatures.

- The solidification structure presents a fairly high homogeneity in the case of sample P1, which

 indicates that during cooling the degree of undercooling ÿTr had corresponding values

 for the development of the diffusion phenomena specific to this alloy and a sufficient degree of homogeneity

 high for the P2 samples, a clear indication that the degree of undercooling ÿTr specific to the process of

 elaboration-casting approached was somewhat higher for the chemical composition of this alloy, with

 a higher degree of alloying.

- Samples P3 and P4 have in common the fact that in their chemical composition the proportion of

 hardly fusible elements (Re, W, Ta). The result is obtaining structures with inhomogeneity

 high chemical and structural, represented by the massive occurrence of dendritic formations.

 Their density and development increases from sample P3 to P4, along with the proportional increase

 of the mentioned elements, clearly proving that the degree of undercooling ÿTr specific

 of the elaboration process was very high.

- Sample P5, with the newly proposed, more economical chemical composition, has a similar structure

 with P2, in the sense that the degree of homogeneity is higher, without being excluded here either

 dendritic formations, more clearly visible at higher magnifications. As a particularity, se

 notices a finer grain, compared to the other investigated samples.

- Along with the increase in the degree of alloying and hard fusible components as part of the composition

   chemical is even more strongly visible in electron microscopes, compared to optical ones, the appearance

 increasingly pronounced dendritic.

- Compositional data provided by point chemical analysis in the interdendritic space

 highlights the reduced amount of Re, confirming the assumption that it concentrates in the axis

 dendrites, less in the interdendritic space.

- Modification of the structure and mechanical properties of INCONEL superalloys developed for

   experiments was possible by applying the mixed heat treatment of tempering for laying

 in solution and aging.

- Heat treatment of INCONEL superalloys with rhenium (Re) significantly influences

   microstructure, mechanical properties and high temperature performance of these alloys.

- One of the main effects of heat treatment on INCONEL superalloys with Re

 is the precipitation and dissolution of secondary phases. Precipitation of secondary phases such as (ÿ')

 and (ÿ"), can significantly improve the mechanical properties of these alloys. For example,

the addition of Re to INCONEL can improve the precipitation behavior of ÿ', which in turn

improves the high temperature resistance of the alloy.

- The heat treatment temperature is a critical factor in the microstructural evolution and in

mechanical properties of INCONEL rhenium superalloys. The proper temperature of

heat treatment can lead to an optimized microstructure and superior properties over time

that inappropriate heat treatment temperatures can cause adverse effects.

Optimizing the heat treatment temperature is essential to achieve the properties

desired for specific applications.

- The heat treatment temperature range for INCONEL superalloys with Re is between

700 and 1200 °C, depending on the specific composition of the alloy and the desired properties. This

temperature range is used for the precipitation of the ÿ' phase, which can improve

creep strength and alloy hardness.

- Optical microscopy of sample P5 after homogenization annealing reveals a structure

fine granular solid solution ÿ. The grain boundaries appear bright, with some noticeable

grouping of precipitated phases, but without being able to precisely establish their nature.

- Hardness after homogenization annealing does not decrease much (from 378 HV02 in the state

cast, at 367 HV02 in homogenized state), confirming also from this point of view that

the homogenization was not total.

- The higher degree of alloying of the P4 alloy changed the structure of the material, even the ratio

between the phase constituents ÿ and ÿ', so that in this case the majority constituent is ÿ'.

The elongated, filiform, bright shapes found in this sample belong to the LAVES phases,

and the increased density can be attributed to the appearance of Mo in the chemical composition, an element which

frequently it can form LAVES phases in INCONEL type alloys.

- In addition to improving the mechanical properties of INCONEL alloys, the addition of Re

it can also substantially increase their corrosion resistance, especially in aggressive environments.

- From the analysis of Tafel curves and corrosion parameters, the following aspects emerge:

- All the curves have very high anodic slopes, which indicates the passivation tendency of the materials;

- The corrosion potentials of the P2-P5 alloys are practically identical, differences of a few tens of mV;

7.2 Original Contributions

- Realization of a complex bibliographic study on superalloys.

- Elaboration and casting in an electric vacuum induction furnace and argon atmosphere of five

types of Inconel alloys, with original chemical composition, of which 4 with variable content of

- The design of a heat treatment technology of elaborated superalloys, which a

including normalizing annealing, solution quenching, aging and explanation

the structural phenomena that occur after each stage;

- Evaluation of hardness variation of worked superalloys by gauges after working and

after each heat treatment operation.

- Structural analysis by optical microscopy of superalloys after elaboration and after

homogenization annealing heat treatments, solution quenching and

getting older.

- Structural and compositional analysis by scanning electron microscopy (SEM)

associated with characteristic X-ray energy dispersive spectroscopy (EDS) a

elaborated superalloys, after casting and homogenization annealing thermal treatments,

solution hardening and aging.

- Analysis of corrosion parameters in H2SO4 solution.

7.3 Future directions of scientific research

- Development in vacuum and argon atmosphere of six nickel base superalloys with

    different chemical compositions;

- The influence of the degree of undercooling and the content of hard fusible elements (Re, W, Ta) on

    the homogeneity of the structure obtained after casting with directed solidification;

- The influence of Mo content on the formation of Laves phases.

In this way, comparative studies can be carried out on the possibility of improving a

physical-mechanical properties and corrosion resistance.

Selective Bibliography

1. D. Locq, A. Walder, M. Marty, P. Caron," Development of New PM Superalloys for High Temperature Applications. EUROMAT, Intermetallics and Superalloys Vol. 10", WILEY-VCH Verlag Gmbh, Weinheim, Germany (DG Morris et al., eds), 2000.

8. Hagel, WC, Wiley, J., "The Superalloys", New York, 1972.

9. Milan T. Jovanoviÿ, Borislav Lukiÿ, Zoran Miškoviÿ, Ilija Bobiÿ, Ivana Cvijoviÿ, Biljana Dimÿiÿ, "Processing and Some Applications of Nickel, Cobalt and Titanium-Based Alloys", Association of Metallurgical Engineers of Serbia.

13. Nageswara Rao Muktinutalapati, "Materials for Gas Turbines - An Overview", VIT University, India.

14. **Grecu,** A, Berbecaru, A, Coman, G, Ciuca S, Matei, E, Sohaciu, M, Gherghescu, I, Predescu, A, Predescu, C, Assessment of premature degradation of a gas injection pipeline due to hydrogen released by the benzene hydrofining equipment, UPB Scientific Bulletin, Series B: Chemistry and Materials Science, olume 85, Issue 2, 2023, p. 257 – 274, FI 0.5;.

18. Maurer, GE, Castledine, W., Schweizer, FA, and Mancuso, S., "Development of HIP Consolidated P/M Superalloys for Conventional Forging to Gas Turbine Components," Superalloys 1996, TMS, Warrendale, PA, 1996, pp. 645–652.

19. Wright, PK, Jain, M., and Cameron, D., "High Cycle Fatigue in a Single Crystal Superalloy:] RG Ding, ZW Huang, HY Li, I. Mitchell, G. Baxter, P. Bowen, Electron microscopy study of direct laser deposited IN718, Mater. Charact., 106 (2015), pp. 324-337,

[25] H. Qi, M. Azer, A. Ritter, Studies of standard heat treatment effects on microstructure and mechanical properties of laser net shape manufactured Inconel 718, Metall. Mater. Trans. A, 40 (10) (2009), pp. 2410-2422

[26] LL Parimi, MM Attallah, JC Gebelin, RC Reed, Direct laser fabrication of Inconel 718: effects on distortion and microstructure, Superalloys, 12th International Symposium on Superalloys, Seven Springs, PA, September 09–13 (2012), pp. 511–519

[27] A. Strondl, R. Fischer, G. Frommeyer, A. Schneider, Investigations of MX and gammaÿ/gammaÿ precipitates in the nickel-based superalloy 718 produced by electron beam melting,

[30] X. Zhao, J. Chen, X. Lin, W. Huang, Study on microstructure and mechanical properties of fast laser forming Inconel 718, Mater. Sci. Eng. A, 478 (1–2) (2008), pp. 119-124

[31] LL Parimi, GA Ravi, D. Clark, MM Attallah, Microstructural and texture development in direct laser fabricated IN718, Mater. Charact., 89 (2014), pp. 102-111

[32] P. Nie, OA Ojo, Z. Li, Numerical modeling of microstructure evolution during laser additive manufacturing of a nickel-based superalloy, Acta Mater., 77 (2014), pp. 85-95

[43] J. Strößner, M. Terock, U. Glatzel, Mechanical and microstructural investigation of nickel based superalloy IN718 manufactured by selective laser melting (SLM), Adv. Eng. Mater., 17 (8) (2015), pp. 1099-1105

[46] NJ Harrison, I. Todd, K. Mumtaz, Reduction of micro-cracking in nickel superalloys processed by selective laser melting: a fundamental alloy design approach, Acta Mater., 94 (2015), pp. 59-68

[53] X. Wang, T. Keya, K. Chou, Build height effect on the Inconel 718 parts fabricated by selective Univ. Technol. Mater. Sci. Ed., 26 (5) (2011), pp. 908-913

[61] S. Raghavan, B. Zhang, P. Wang, CN Sun, MLS Nai, T. Li, J. Wei, Effect of different heat treatments on the microstructure and mechanical properties in selective laser melted Inconel 718 alloy, Mater. Manuf. Process., 32 (14) (2017), pp. 1588-1595

[62] VA Popovich, EV Borisov, AA Popovich, VS Sufiiarov, DV Masaylo, L. Alzina, Functionally graded Inconel 718 processed by additive manufacturing: crystallographic texture, anisotropy of microstructure and mechanical properties, Mater. Des., 114 (2017), pp. 441-449

[66] E. Amsterdam, GA Kool, High cycle fatigue of laser beam deposited Ti-6Al-4V and Inconel 718, MJ Bos (Ed.), Proceedings of the 25th Symposium of the International Committee on Aeronautical Fatigue, Rotterdam, The Netherlands, 27–29 May, Springer Netherlands, Dordrecht (2009), pp. 1261-1274

[73] D. Deng, RL Peng, Håkan Brodin, J. Moverare, Microstructure and mechanical properties of inconel 718 produced by selective laser melting: Sample orientation dependence and effects of post heat treatments, Mater. Sci. Eng. A, 713 (2018), pp. 294-306

[77] WM Tucho, P. Cuvillier, A. Sjolyst-Kverneland, V. Hansen, Microstructure and hardness studies of Inconel 718 manufactured by selective laser melting before and after solution heat treatment, Mater. Sci. Eng. A, 689 (2017), pp. 220-232

[85] JP Choi, GH Shin, S. Yang, DY Yang, JS Lee, M. Brochu, JH Yu, Densification and microstructural investigation of Inconel 718 parts fabricated by selective laser melting, Powder Technol., 310 (2017), pp. 60-66

[86] R. Acharya, JA Sharon, A. Staroselsky, Prediction of microstructure in laser powder bed fusion process, Acta Mater., 124 (2017), pp. 360-371

[89] W. Sames, PhD Thesis: Additive Manufacturing of Inconel 718 Using Electron Beam Melting: Processing, Post-Processing and Mechanical Properties (2015)

[90] MM Kirka, F. Medina, R. Dehoff, A. Okello, Mechanical behavior of post-processed Inconel 718 manufactured through the electron beam melting process, Mater. Sci. Eng. A, 680 (2017), pp. 338-346

[91] D. Deng, Licentiate Thesis: Additively Manufactured Inconel 718: Microstructures and Mechanical Properties, Linköping Studies in Science and Technology (2018)

[92] F. Brenne, A. Taube, M. Pröbstle, S. Neumeier, D. Schwarze, M. Schaper, T. Niendorf,
Microstructural design of Ni-base alloys for high-temperature applications: impact of heat treatment
on microstructure and mechanical properties after selective laser melting, Prog. Add. Manuf., 1 (3)
(2016), pp. 141-151

[95] T. Trosch, J. Strößner, R. Völkl, U. Glatzel, Microstructure and mechanical properties of
selective laser melted Inconel 718 compared to forging and casting, Mater. Lett., 164 (2016), pp.
428-431

[99] X. Wang, K. Chou, Residual stress in metal parts produced by powder-bed additive
manufacturing processes, Proceedings of the 26th Annual International Solid Freeform Fabrication
Symposium – An Additive Manufacturing Conference, Austin, Texas, August 10–12 (2015), pp.
1463-1474

[100] B. Baufeld, Mechanical properties of Inconel 718 parts manufactured by shaped metal
deposition (SMD), J. Mater. Eng. Perform., 21 (7) (2012), pp. 1416-1421

[104] O. Scott-Emuakpor, J. Schwartz, T. George, C. Holycross, C. Cross, J. Slater, Bending fatigue
life characterization of direct metal laser sintering nickel alloy 718, Fatigue Fract. Eng. Mater.
Struct., 38 (9) (2015), pp. 1105-1117

[110] F. Liu, X. Lin, G. Yang, M. Song, J. Chen, W. Huang, Microstructure and residual stress of
rapid laser formed Inconel 718 nickel-base superalloy, Optics Laser Technol., 43 (1) (2011), pp.
208-213

[111] T. Mukherjee, W. Zhang, T. DebRoy, An improved prediction of residual stresses and
distortion in additive manufacturing, Comput. Mater. Sci., 126 (2017), pp. 360-372

[112] Reed R., 2008. The Superalloys Fundamentals and Applications, 1st Edition. Cambridge
University Press (Ed.), New York, pp. 1-372.

[120] T. Wanga, H. Zhanga, C. Liud, X. Gongb, Y. Peib, Y. Zoue, Y. Liua, Q. Wanga - Effect of
temperature on tensile behavior, fracture morphology and deformation mechanisms of Nickel-based
single crystal CMSX-4, Journal of Alloys and Compounds, Volume 912, 15 August 2022, 165175

[121] H. Zhang, Q. Wang, X. Gong, T. Wang, W. Zhang, K. Chen, C. Wang, Y. Liu, Q. Wang,
Dependence on temperature of compression behavior and deformation mechanisms of nickel-based
single crystal CMSX-4, J. Alloy. Compd. 866 (2021) 158878.

[128] Nicolae, A., Duma, RM, Gradinaru, C., **Grecu, A.,** Ciucÿ, S., Nicolae, M., New scientific
branches of the sustainable-durable development in the metallic materials engineering, UPB
Scientific Bulletin, Series B: Chemistry and Materials Science, 2021, 83(4), pp. 223–228, FI 0.5;

[132] Titi Dulÿmita, Emil Florian "Thermal and thermochemical treatments", Didactic Publishing House and
Pedagogy, 1983.

[133] **Grecu, A.,** Coman, G., Berbecaru, A., Matei, E, Gherghescu, I, Predescu, A, Ciuca, S,
Influence of mechanical characteristics on the operating behavior of compressors intake and exhaust

valves made of inconel x750 superalloy, UPB Scientific Bulletin, Series B: Chemistry and Materials Science, 2023, 85(1), pp. 177–188, FI 0.5;

[134] Grÿdinaru, C.ÿ., Pantilimon, MC, **Grecu, A.,** Predescu, C., Nicolae, A., E, Eco-socio technological degradation of the metallic materials, UPB Scientific Bulletin, Series B: Chemistry and Materials Science, 2022, 84(2), pp. 155–164, FI 0.5;

[135] Grÿdinaru, C.ÿ., Coman, G., Ciucÿ, **S., Grecu, A.,** Gherghescu, IA, Research on corrosion degradation process of some thermal power plants steam boiler pipes, UPB Scientific Bulletin, Series B: Chemistry and Materials Science, 2021, 83(3), pp. 231–244, FI 0.5;

[136] Pantilimon, Mircea Cristian; Berbecaru, Andrei; Gherghescu, Ioana; Coman, George; Chuk, Sorin; **Grecu, Andrei;** Sohaciu, Mirela Gabriela; Dumitrescu, Ruxandra Elena; Predescu, Cristian; Comparative evaluation of the trip effect in steels with different contents of mn and al; Metals; Volume 12; Issue 3; March 2022; WOS:000774103200001, FI 2.9.